Journal of Sedimentary Research

Journal of Sedimentary Research, 2006, v. 76, 292–309
Research Article
DOI: 10.2110/jsr.2006.028

PALUSTRINE DEPOSITS ON A LATE DEVONIAN COASTAL PLAIN—SEDIMENTARY ATTRIBUTES AND IMPLICATIONS FOR CONCEPTS OF CARBONATE SEQUENCE STRATIGRAPHY

ALEX J. MacNEIL AND BRIAN JONES
Department of Earth and Atmospheric Sciences, 1-26 ESB, University of Alberta, Edmonton, AB T6G 2E3 CANADA
e-mail: ajm2@ualberta.ca

ABSTRACT: **Palustrine deposits in coastal environments can cover thousands of square kilometers and are stratigraphically important. Palustrine deposits that originated in supratidal marshes can be used to track shifts in the shoreline position, whereas palustrine deposits that formed in marshes above the peritidal realm are indicative of subaerial unconformities. Despite the importance of these deposits, there are few documented examples of ancient coastal palustrine deposits, and their sedimentary attributes remain poorly understood. Misinterpretation of coastal palustrine deposits as marine deposits, or calcrete, may partly explain this situation.**

The Upper Devonian Alexandra Formation, exposed in the Northwest Territories of Canada, is formed of two reef complexes that are separated by a Type I sequence boundary. At the landward part of the platform, this boundary is marked by a succession of coastal-plain deposits that is ~ 50 cm thick. The most distinct aspect of this succession are palustrine deposits characterized by charophytes, skeletal (*Rivularia*) stromatolites, and various pedogenic features including complex crack networks, root traces, and authigenic kaolinite. Karst features and calcrete, generally regarded as typical indicators of subaerial exposure, are not found.

This study highlights the sedimentary attributes that can be used to identify ancient palustrine deposits in marine coastal regions, distinguish these deposits from calcrete, and demonstrates their sequence stratigraphic significance, when found in marine limestone successions. It clearly demonstrates that palustrine deposits, like those found in the Alexandra Formation, should be considered indicative of subaerial unconformities and sequence boundaries, in the same manner as karst and calcrete.

INTRODUCTION

Palustrine carbonates are fresh- to brackish-water deposits, with evidence of pedogenesis, that are typically deposited around the margins of lakes (Freytet 1973; Freytet and Plaziat 1982; Alonso-Zarza 2003). If climate permits, they can also form in shallow, carbonate-rich, fresh- to brackish-water marshes established on coastal plains and supratidal flats (Monty and Hardie 1976; Shinn 1983; Platt and Wright 1992). In these marginal marine settings, palustrine deposits can cover thousands of square kilometers, and may co-occur with karst and calcrete (Platt and Wright 1992). As such, the presence of palustrine deposits in successions of ancient marine limestones has important stratigraphic utility because they may indicate shifts in the shoreline position (cf. Monty and Hardie 1976) and the position of a sequence boundary. Nevertheless, few examples of such deposits have been documented from ancient marine limestone successions, possibly because they have been mistaken for marine deposits or calcrete (cf. Monty and Hardie 1976; Wright 1985). As a result, their potential importance to sequence stratigraphy has been overlooked.

The Upper Devonian Alexandra Formation (< 40 m thick), located in the Northwest Territories of Canada (Fig. 1), is formed of two reef complexes that developed on an epicontinental ramp (MacNeil and Jones in press). The second reef complex developed on the outer ramp after development of the first reef complex, located on the inner ramp, was terminated by a drop in sea level. The top of the limestones that had been deposited on the inner ramp formed the base of the coastal plain to the second reef complex, and through subaerial weathering became stained black and red. Subsequent establishment of fresh- to brackish-water marshes on the coastal plain led to deposition of palustrine carbonates that are dominated by charophytes and skeletal stromatolites. Pedogenic features in these deposits include root traces partly filled with vadose silts and authigenic kaolinite, complex crack networks that impart a nodular texture, and zoned calcite fabrics that resemble the alpha fabrics found in some calcretes (Wright 1988; Wright and Peeters 1989). The palustrine carbonate was then buried by a marine limestone derived from a short-lived marine incursion. Following retreat of the shoreline, these deposits were also subjected to subaerial exposure and pedogenesis. Weathering of these deposits was terminated by retrogradation of peritidal environments of the second reef complex. As such, marine limestone deposits of the two reef complexes are separated by a succession of unconformable coastal-plain deposits that is ~ 50 cm thick.

In contrast to the development of well-defined karst features or pedogenic calcrete profiles, regarded as typical indicators of subaerial unconformities and sequence boundaries (e.g., James 1972; Esteban and Klappa 1983; Sarg 1988; Handford and Loucks 1993), the coastal-plain deposits in the Alexandra Formation, and their evidence of subaerial exposure and pedogenesis, are subtle. Nonetheless, they represent a Type I sequence boundary, and its recognition is critical to understanding the depositional evolution and stratigraphic framework of the entire reef system. This study examines the sedimentology of the coastal-plain deposits and the evidence of pedogenesis, and presents an enhanced set of

 1527-1404/06/076-292/$03.00

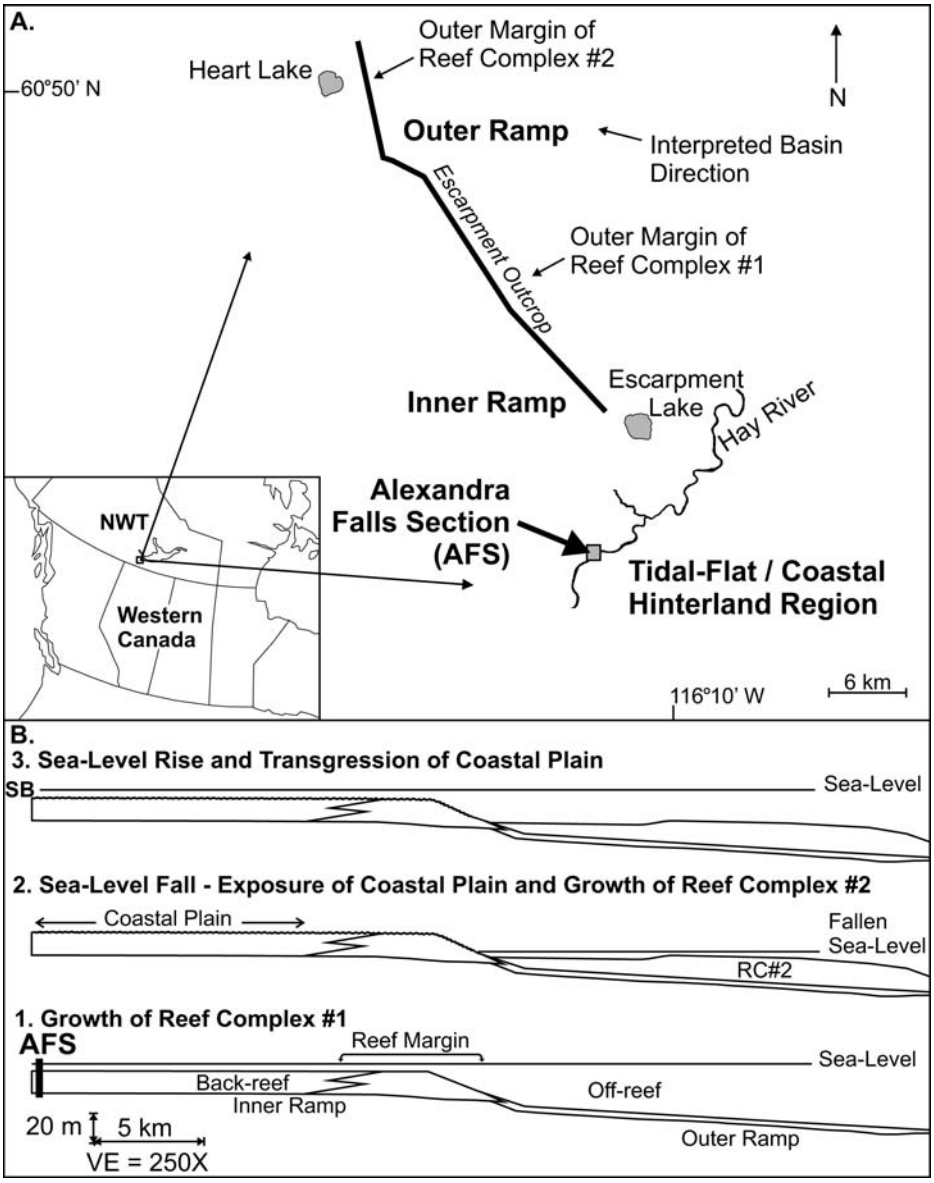

FIG. 1.—Study area and simplified stratigraphic evolution of the Alexandra Formation. **A)** Locality map of the Alexandra Formation. **B)** Three-stage evolution of the reef system in the Alexandra Formation. Section orientation from Alexandra Falls at left to Heart Lake at right. AFS = Alexandria Falls Section; SB = Sequence Boundary.

criteria for the recognition of ancient palustrine deposits. These deposits in successions of marine limestones should be considered indicative of subaerial unconformities and sequence boundaries in the same manner as calcrete and karst, underscoring their importance to carbonate sequence stratigraphy.

GEOLOGICAL SETTING

The Alexandra Formation is exposed along a southwest–northeast gorge system cut by the Hay River and in a southeast–northwest trending escarpment (Fig. 1A). Regional biostratigraphy indicates that these deposits are mid-Frasnian in age (Klapper and Lane 1985; McLean and Klapper 1998). Strata along Hay River were deposited at the landward extent of an epicontinental ramp and show little lateral variation because the exposure trend is nearly parallel to depositional strike. In contrast, the escarpment is oblique relative to depositional strike, providing a nearly continuous section through strata deposited in back-reef, reef, and fore-reef environments (e.g., Jamieson 1967). Detailed study of the formation over the summers of 2002 and 2003 determined that these deposits belong to two separate reef complexes (MacNeil and Jones in press). The first Reef Complex (RC#1) developed on the inner ramp in a highstand systems tract, after an initial transgression, whereas the second, younger Reef Complex (RC#2) developed basinward of RC#1, after sea level fell (Fig. 1B). Deposition of shallow restricted subtidal and intertidal facies on the outer ramp, directly above fore-reef deposits of the first reef complex, indicate that (1) a fall in sea level terminated development of RC#1 on the inner ramp, and (2) the magnitude of sea level fall, based on stratigraphic correlation, was ~ 17 m. As such, development of RC#2 in a lowstand systems tract was fringed by a low-relief coastal plain developed at the top of RC#1 (Fig. 1B #2). The coastal-plain succession at the top of RC#1, and a subtidal correlative conformity at the base of RC#2, separates deposits of the two reef complexes and defines a Type I sequence boundary (following definition of Posamentier and Vail (1988), whereby the subaerial unconformity formed due to a fall in relative sea level). Exposure of the boundary is continuous for at least 500 m in the cliff faces below Alexandra Falls along Hay River (Fig. 2A), although previous study failed to recognize its unconformable nature (e.g., Belyea and McLaren 1962; Jamieson 1967; Bellow 1993). A subsequent sea-level

rise flooded RC#2 and led to transgression of the coastal plain and deposition of peritidal facies (Fig. 1B #3).

METHODS

The sequence boundary exposed in the cliff faces below Alexandra Falls is difficult to access because the vertical cliffs are ~ 35 m high. Only one locality (Alexandra Falls Section; AFS) was found where the boundary could be safely accessed (Fig. 2A). Two profiles through the boundary, CS1 and CS2, ~ 15 m apart, were measured at this locality (Fig. 2B, C). Large samples (n = 12) were collected from these sections, and large (5 cm × 7.5 cm) thin sections (n = 15) were prepared from these for transmitted-light microscopic examination. In addition, small pieces fractured from selected samples (n = 4), polished thin sections (n = 2) etched for 45 s in 50% acetic acid, and polished and etched chip samples (n = 3) were coated with Au and examined with a JEOL 6301 field emission scanning electron microscope (SEM). Each of these sample preparation methods facilitated a different, but complementary, perspective of the features examined with the SEM. A Princeton Gamma-Tech Energy Dispersive X-ray Analyzer, operated at an accelerating voltage of 20 kV, was used with the SEM to identify calcite, feldspar, gypsum, and clay minerals. X-ray diffraction (XRD) analysis of powdered samples (n = 6) was used to confirm mineral identifications. Back-scattered electron (BSE) images of selected samples were collected with a JEOL 8900R electron microprobe operated at 15 kV accelerating voltage. The classification scheme of Folk (1959) for the size of micrite (1–4 μm), microspar (5–15 μm), and sparite (> 15 μm) is utilized.

STRATIGRAPHIC SUCCESSION

Sections CS1 and CS2 contain the same stratigraphic units with no discernible difference in bed thickness, with exception of the palustrine deposit, which varies from 10 to 20 cm thick. Four units have been recognized (Fig. 2B, C). The lowest, termed the host limestone, is the succession (13.6 m thick) of shallow marine and peritidal deposits from the lagoon and tidal-flat region of RC#1. The top of this unit marks the top of RC#1. Unit 2 is the palustrine deposit. Unit 3 is the short-lived marine incursion deposit, ~ 35 cm thick. Unit 4 is the overlying succession (7 m thick) of peritidal deposits that belong to RC#2.

PRIMARY SEDIMENTOLOGY OF UNITS 1–4

Unit 1—Host Limestone

The lagoonal and peritidal deposits of RC#1 include bedded *Amphipora* deposits, peloidal packstones, laminated mudstones, and intertidal stromatolites, commonly in shallowing-upward cycles. Cloudy rhombs (~ 20 μm) of dolomite are found locally.

The top of Unit 1 is a thick bed of *Amphipora*-dominated floatstone–rudstone with a wackestone matrix. Its uppermost ~ 40 cm is irregularly stained black and red by Fe-sulfides, Fe-oxides, and derived pigments. Clotted and disseminated finely crystalline Fe-oxides are common in freshly broken samples, imparting a distinct red color to many *Amphipora* (Fig. 2D). Other *Amphipora* are partly impregnated with Fe-sulfides, resulting in a blackened stain to their appearance.

Unit 2—The Palustrine Deposit

Sharply overlying Unit 1 is a recessive, brown wackestone with a nodular-chalky texture (Fig. 2E). Variably calcified charophyte stems, gyrogonites, and hollow calcite spheres are common throughout this unit. Distinct amber-colored laminated microbial calcite precipitates that form shrub-like masses, up to 2 mm thick, are found locally. Blackened lithoclasts and abraded, poorly preserved fragments of *Amphipora*, always with some degree of Fe-sulfide impregnation, are present in minor amounts (Fig. 3A, B). These are most probably derived from weathering of the underlying blackened *Amphipora* floatstone–rudstone. Detrital quartz is present in minor (< 5%) amounts. No dolomite was found in this unit.

The charophytes (Fig. 3C) are characterized by brown-amber colored, inclusion-rich crystals, commonly with lamellar growth structure. Some charophytes were recrystallized and their primary morphological features are nearly indiscernible (Fig. 3D). Micrite in the deposit is characterized by inclusion-rich calcite comparable to the calcified charophytes, suggesting that much of it may have originated from charophyte degradation. The hollow calcite spheres include small spheres with outer diameters ≤ 10 μm and large spheres with inner diameters of 15–20 μm and outer diameters of 25–40 μm (Fig. 3D–F). Wall structure of the small spheres is characterized by a layer of blocky, anhedral calcite. Wall structure of the larger spheres is characterized by either a layer of blocky, anhedral calcite, or a radial arrangement of bladed crystals. Unfortunately, because hollow calcitic spheres have several possible origins (e.g., Jones 1992; Guo and Riding 1992), the affinity of these spheres is unknown.

The amber-colored laminated calcitic precipitates are characterized by lensoid to hemispherical shrub-like shapes in longitudinal section, up to 2 mm high, or fragmented pieces of these masses (Fig. 4). Parallel to slightly curved branching tubules, ~ 10 μm in diameter, are well defined in these structures (Fig. 4A, B). The calcite between the tubules is thinly (submicron–micron scale) laminated with light and dark layers and very fine inclusions (Fig. 4C). Branching of the tubules always takes place near the terminal surface of the precipitates (Fig. 4D). In transverse section, the precipitates have a honeycomb-like appearance (Fig. 4E). These features are consistent with microbial precipitates (e.g., Riding 2000) but are not similar to any known marine microbial precipitate from the Paleozoic (cf. Pratt 1984; Riding 1991, 2000). Rather, they are directly comparable to modern freshwater skeletal stromatolites (Freytet and Plet 1996; Freytet and Verrecchia 1998) and, in particular, *Rivularia* skeletal stromatolites, which have a fossil record extending back to the Precambrian (Bertrand-Sarfati 1976; Golubic et al. 2000). Modern examples of freshwater *Rivularia haematites* stromatolites, for example, are characterized by (1) masses of calcified, nearly parallel filaments of comparable diameters, (2) synchronous events of false branching at the outer margins of colonies, (3) thinly laminated sparitic calcite between filaments, and (4) a honeycomb appearance of colonies in transverse section (e.g., Monty 1976; Pentecost 1978, 1987; Freytet and Verrecchia 1998; Caudwell et al. 2001; Pentecost and Edwards 2003). The microbial precipitates in Unit 2 display these characteristics. Fragmented pieces of these microbial precipitates and disarticulated, fragmented charophytes are abundant throughout the matrix of Unit 2 (Fig. 4B, F).

→

Fig. 2. Exposure of coastal-plain succession in Alexandra Formation along Hay River. A–C and E = field photographs; D = photograph of polished surface. **A)** Alexandra Formation exposed in cliff faces below Alexandra Falls. Top contacts of RC#1 and RC#2 are sharp and traceable across field of view. AFS = Alexandra Falls Section. Cliff height ~ 35 m, view to southwest. **B)** CS1 at AFS. Arrows indicate contacts between units. Note recessive nature of Units 2 and 3, relative to Units 1 and 4. **C)** CS2 at AFS. Arrows indicate contacts between units. **D)** *Amphipora* floatstone from top of Unit 1 at CS2. *Amphipora* are stained red and matrix is partly stained (S). **E)** Sharp contact at base and top of Unit 2 at CS1.

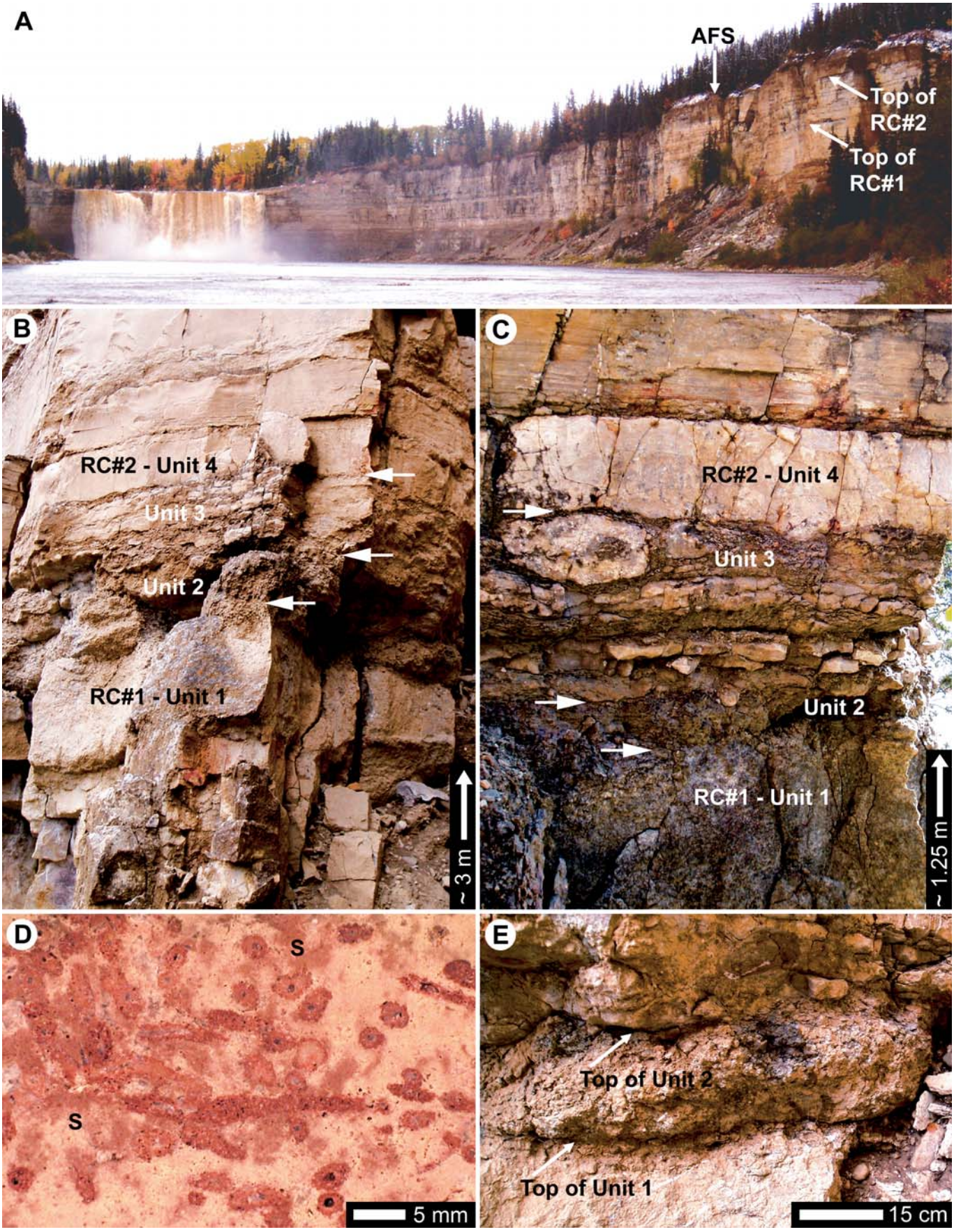
A
AFS
Top of RC#2
Top of RC#1
B
RC#2 - Unit 4
Unit 3
Unit 2
RC#1 - Unit 1
~ 3 m
C
RC#2 - Unit 4
Unit 3
Unit 2
RC#1 - Unit 1
~ 1.25 m
D
S
S
5 mm
E
Top of Unit 2
Top of Unit 1
15 cm

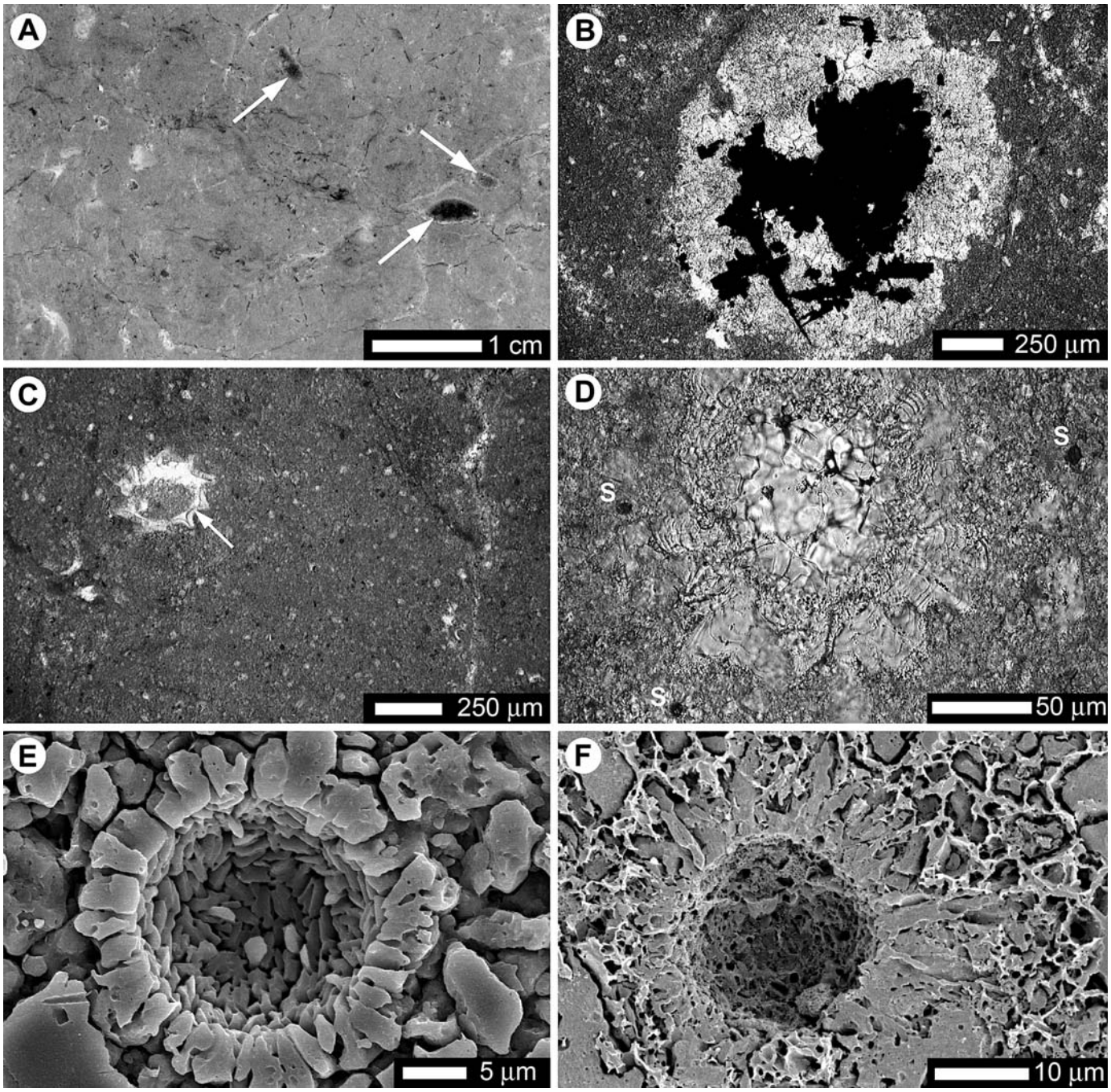

FIG. 3.—Depositional features in Unit 2. A = photograph of polished surface; B–D = thin section photomicrographs; E, F = SEM photomicrographs. **A)** Blackened lithoclasts (arrows) in Unit 2 that were derived from top of Unit 1. **B)** Poorly preserved *Amphipora* fragment with clotted Fe-sulfides that was derived from top of Unit 1. **C)** Charophyte gyrogonite (arrow). Abundant small pieces of fragmented charophytes impart speckled appearance to matrix. **D)** Intensely recrystallized charophyte with lamellar crystal structure. Note hollow spheres (S) in matrix. **E)** Hollow sphere with wall formed of blocky micrite. **F)** Hollow sphere with wall constructed of bladed calcite crystals (etched sample).

Charophytes in modern freshwater environments are closely associated with microbes and their precipitates (e.g., Freytet and Plaziat 1982; Platt and Wright 1992), and in particular *Rivularia* (Whitton 1987). Thus, interpretation of these microbial precipitates as *Rivularia* skeletal stromatolites is consistent with the abundance of charophytes in the unit. The combination of charophytes and microbial precipitates, without any associated marine biota (e.g., *Amphipora* that do not occur as detrital, Fe-stained clasts derived from the top of Unit 1, calcispheres *sensu* Williamson (1880), foraminifera, marine algae, or *Stachyodes*—all of which are abundant in the underlying and overlying marine limestones) indicates that Unit 2 was deposited in a shallow, fresh- to brackish-water environment. The absence of any dolomite, which is unlikely to be formed from fresh and brackish waters (Hardie 1987), but is a common primary precipitate in peritidal facies throughout the formation, supports this interpretation. The lack of marine sediment mixed in with Unit 2, or laminated alternations between fresh-water-derived and marine-water-derived sediment, further indicates that these deposits were disconnected from the marine realm (cf. Monty and Hardie 1976).

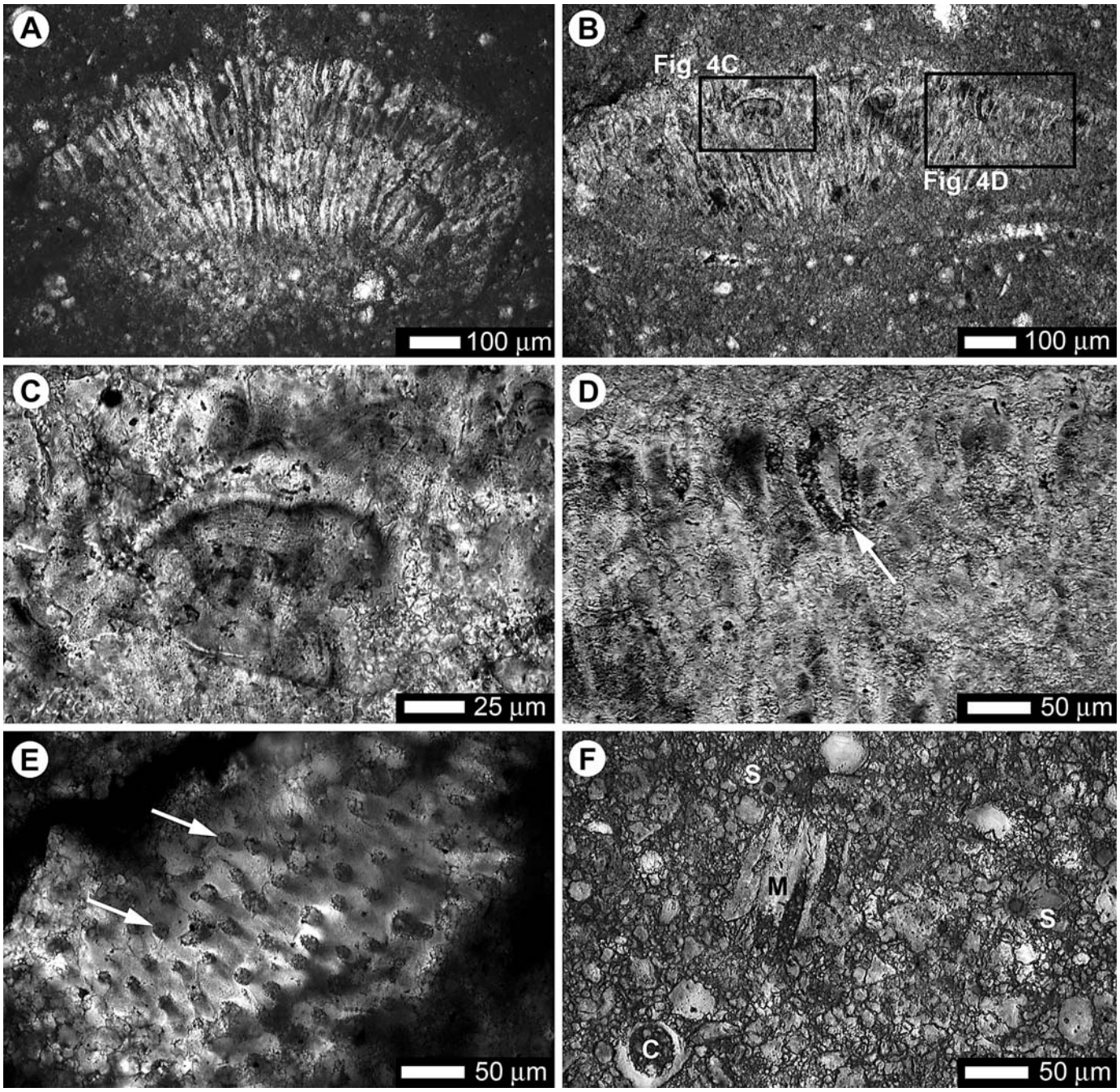

FIG. 4.—Thin-section photomicrographs of skeletal stromatolites in Unit 2. **A, B)** Well-preserved skeletal stromatolites in matrix. Boxes in Figure 4B indicate positions of figure parts C and D. **C)** Laminated light and dark spar between tubules, near terminal growth surface. **D)** Falsely branched tubule (arrow) near terminal growth surface. **E)** Transverse surface of skeletal stromatolite with honeycomb appearance. Two tubules are indicated with arrows. **F)** Matrix with numerous hollow spheres (S) and fragmented pieces of charophytes (C) and skeletal stromatolites (M).

Unit 3—The Marine-Incursion Deposit

The boundary between Unit 2 and overlying Unit 3 is well defined but irregular (Fig. 2E). Unit 3 is a dark gray limestone with numerous *Amphipora* along with fewer ostracods and scattered fragments of corals, stromatoporoids, and brachiopods. Detrital quartz is present in the matrix in minor (< 5%) amounts, along with ripped-up clasts of Unit 2 (Fig. 5A). The latter indicates partial erosion of the palustrine deposit prior to (or during) deposition of Unit 3. The biota of this unit is consistent with a shallow marine facies that was periodically supplied-with storm-derived detritus. The fragments of corals and stromatoporoids show evidence of extensive transport and abrasion, relative to the *Amphipora*, indicating they were not locally derived. The deposit probably represents a marine incursion over the coastal plain with periodic storm transport of allochthonous reef-derived detritus.

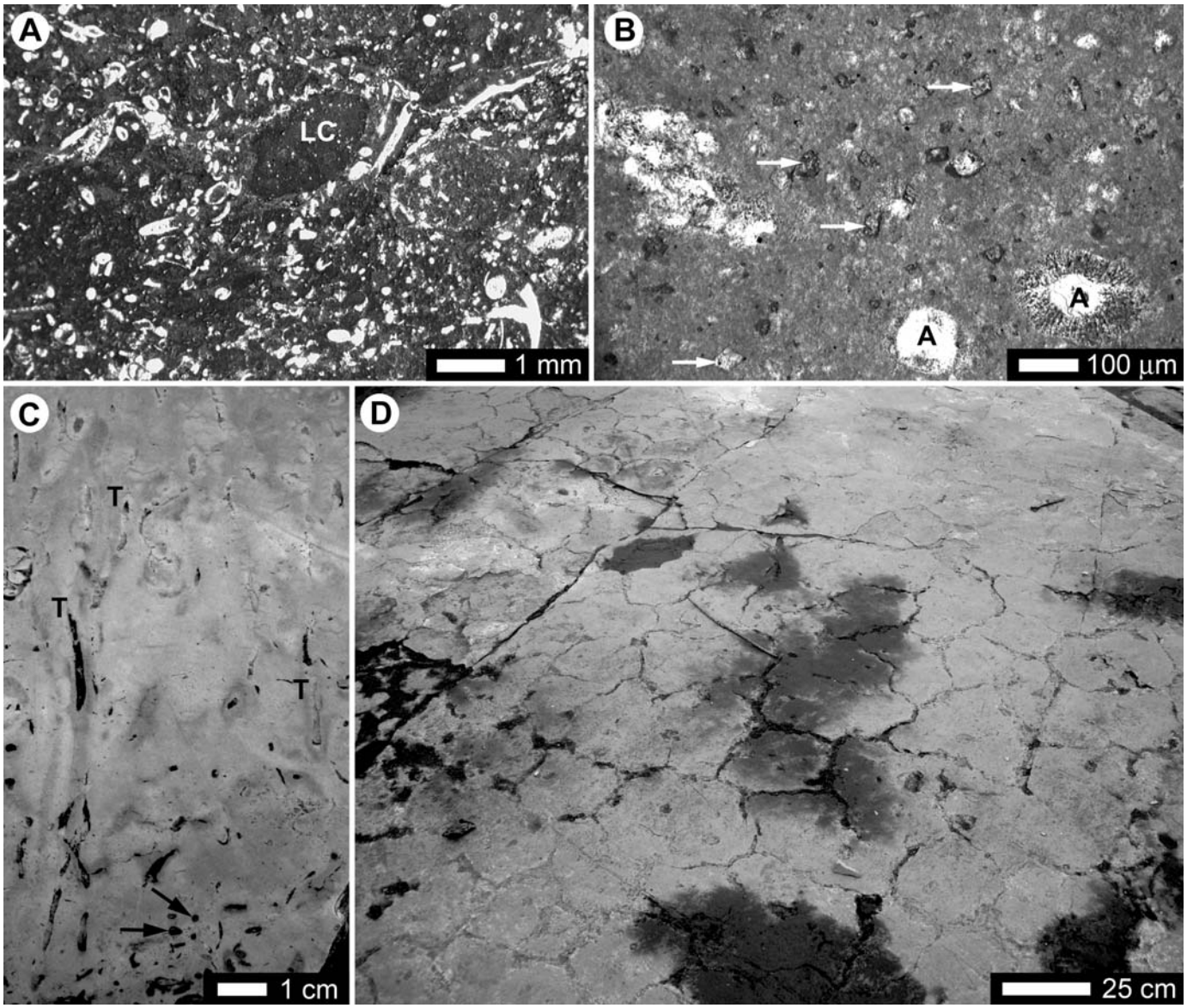

FIG. 5.—Depositional features of Unit 3 and Unit 4. A, B = thin-section photomicrographs; C = photograph of polished surface; D = field photograph. **A)** Unit 3 matrix with abundant algal fragments and ripped-up Unit 2 lithoclast (LC). **B)** Wackestone in Unit 4 with algal fragments (A) and yellowish rhombs of syndepositional dolomite scattered throughout (some indicated with arrows). **C)** Sample from bed at base of Unit 4 showing spar-filled vertically elongated tubules (T). *Amphipora* fragments at base of sample (arrows). **D)** Exposed bedding plane in Unit 4 with well-preserved mudcracks.

Unit 4—Peritidal deposits of RC#2

Unit 3 is sharply overlain (Fig. 2B) by well-bedded deposits (0.2–1.1 m thick) of Unit 4 that extend to the top of the Alexandra Formation (Fig. 2A). The basal deposit is a burrowed, light tan algal mudstone–wackestone with numerous palaeoberesellids, *Vermiporella*, and ostracods. *Amphipora* are less common. Yellowish primary dolomite is common throughout the matrix (Fig. 5B). Spar-filled vertical tubes, analogous to those described from Ordovician, Cretaceous, and modern supratidal storm deposits by Shinn (1983), are conspicuous (Fig. 5C). This bed, and overlying beds, characterized by mudstones and shallowing-upward peritidal deposits, lack evidence of pedogenesis, although many bedding planes display mudcracks and desiccation breccias (Fig. 5D). The deposits in Unit 4 are interpreted as peritidal deposits that belong to RC#2.

FEATURES OF SUBAERIAL EXPOSURE AND PEDOGENESIS

Unit 1—The Host Limestone

Evidence of subaerial exposure and pedogenesis in Unit 1 is limited because karst features such as vuggy porosity, or calcrete deposits, are not found. The only evidence of subaerial exposure is the Fe-staining in its uppermost ~ 40 cm, and the impregnation of *Amphipora* with clotted Fe-sulfides and Fe-oxides (Fig. 2D). Because blackened lithoclasts and stained *Amphipora* fragments were incorporated into Unit 2, the cause of staining must have pre-dated establishment of marsh-like conditions on the coastal plain.

Although blackened limestones may be produced in anoxic subtidal environments (Strasser 1984), this mechanism is discounted for explaining the staining at the top of Unit 1 because (1) the same depositional facies, without staining, is common lower in the unit, (2) it lacks mudstone,

vertical fenestrae, or dark muddy deposits, which may indicate the deposit underwent a period of subtidal stagnation, (3) similar facies are found in Unit 4, without staining, and (4) the staining at the top of Unit 1 directly underlies an unconformity. The staining, therefore, is attributed to subaerial exposure and a series of diagenetic processes similar to those documented from recent and Cretaceous coastal plains by Strasser (1984), Shinn and Lidz (1988), and Vera and de Cisneros (1993). Blackening of exposed limestones on coastal plains, through processes that may include adsorption of organics, staining by Fe-sulfides, and fires (Shinn and Lidz 1988), is characterized by irregular patterns of staining and blackened intraclasts (Strasser 1984), like those present at the top of Unit 1. Extensive black and red staining has also been documented as an alteration feature found at the subaerial unconformity that defines the top of the Mississippian Monteagle Limestone Formation, in the United States (Driese et al. 1994). The preferential staining of *Amphipora* fragments at the top of Unit 1 is akin to the preferential blackening of Pleistocene corals in Florida, attributed by Strasser (1984) to the percolation of staining fluids through their porous skeletons.

Unit 2—The Palustrine Deposit

Features in Unit 2 indicative of subaerial exposure and pedogenesis include complex horizontal, vertical, and curved crack networks, and root traces lined and filled with various materials. Other features, including zoned neomorphic calcite crystals, calcite crystals with matrix embayments and authigenic clay inclusions, and spherulites, are more enigmatic but comparable to pedogenic features found in calcretes.

Crack Networks and Development of a Nodular Texture.—Throughout Unit 2 there are submillimetric horizontal, vertical, and curved cracks. Some of the horizontal and vertical crack networks are associated with small-scale brecciation (Fig. 6A), and the curved crack networks give the rock a nodular texture which is evident in outcrop and thin section. Micrite, authigenic kaolinite, illite, and/or calcite cement fill or partly fill the cracks and brecciated zones. Similar crack networks in palustrine carbonates and calcretes have been attributed to drying of soft but cohesive sediment, presumably repeated numerous times before lithification took place (e.g., Freytet 1973; Freytet and Plaziat 1982; Braithwaite 1983; Platt 1989; Tandon and Friend 1989; Alonso-Zarza 2003).

Root Traces.—Root traces in Unit 2 are characterized by vertical and subhorizontal sinuous tubes, 1–2 mm in diameter, generally $<$ 2 cm in length, that bifurcate locally (Fig. 6B–D). Where these traces are intersected by crack networks, they have become brecciated into irregular fractures and vugs (Fig. 6D).

The voids formed by the root traces and their brecciated equivalents are filled by various materials. Many voids contain calcitic vadose silt (Fig. 6D–F), characterized by micrite and microspar grade anhedral, clear calcite crystals (cf. Dunham 1969; Freytet and Plaziat 1982; Platt 1989; Jones and Kahle 1995). Calcite silt is also found in some voids at constrictions, and in rare cases contains bifurcating segmented root hairs or fungal hyphae (mycorrhizae?) that are preserved by iron oxides (Fig. 6F).

Clay cutans and dense micritic coatings of variable thickness also partly line many voids (Fig. 7A–D). The micritic coatings appear to be calcitic cutans or the products of void-lining biofilms (Fig. 7A). Many are formed of micrite–clay mixtures (Fig. 7B), and many coatings have partly or completely spalled off, forming clasts (Fig. 7C). Some linings include calcite spherulites (Fig. 6F), which are common in void-lining cutans (Brewer 1964). Spalling of the linings is attributed to expansion and constriction of the surrounding matrix due to periodic wetting and drying, akin to the generation of the crack networks.

Some voids also contain coarse, inclusion-rich calcite rhombs (comparable with the intercalary crystals of Brewer (1964)) mixed in with vadose silt (Fig. 7C, D), and books of authigenic kaolinite arranged into vermiform patterns (Fig. 7D–F). Root traces and brecciated, modified root traces, partly lined and filled with vadose silt, authigenic clays, cutans, and coarse calcite crystals, have been well documented as pedogenic indicators in other palustrine carbonate deposits (e.g., Freytet 1973; Freytet and Plaziat 1982; Platt 1989; Dunagan and Driese 1999; Alonso-Zarza 2003) and in many calcretes (e.g., Bal 1975; Wieder and Yaalon 1974, 1982; Braithwaite 1983; Esteban and Klappa 1983; Drees and Wilding 1987).

Spar Patches, Neomorphic Calcite, and Authigenic Minerals.—Randomly distributed throughout Unit 2 are small ($<$ 1 mm), irregular-shaped patches of spar that in some parts appear transitional with the surrounding micritic matrix (Fig. 7G). The transition zones appear to be aggradationally recrystallized micrite with the degree of aggradation increasing towards the spar patch (cf. Folk 1959). Inclusions of matrix in the crystals and matrix embayments are common. These patches are similar to crystallaria, nodules, and crystal tubes described from other palustrine carbonates, calcretes, and soils (e.g., Brewer 1964; Freytet 1973; Wieder and Yaalon 1974, 1982; Braithwaite 1983; Tandon and Friend 1989; Purvis and Wright 1991), which are generally attributed to complex neomorphic processes involving dissolution of micrite in the matrix at the expense of the precipitating spar (cf. Brewer 1964; Sehgal and Stoops 1972; Freytet 1973; Tandon and Friend 1989; Purvis and Wright 1991). Similar neomorphic processes in Unit 2 may explain these patches that are at least partly transitional with the surrounding matrix.

Light-colored zoned calcite crystals are found in and around the spar patches, and in the matrix of Unit 2, in some cases as overgrowths on micrite (Figs. 7H, 8A–D). In many cases, micrite and clays, some of which were authigenic, have been trapped as inclusions in the crystals (Fig. 8B, D). The crystals in the matrix, generally of microspar grade, vary in shape from rhombic with planar faces and straight edges to anhedral forms with curved faces and irregular boundaries. Concentric growth zones are well defined. Some crystals intersect each other or grow in jagged forms. Many zoned crystals also have fine tubule inclusions (Fig. 8A), consistent with precipitation or neomorphism in the presence of filamentous microbes. The size range of tubule inclusions is variable, indicating that more than one taxon of microbe was present (e.g., cyanobacteria, fungi). In rare cases, filaments extending from crystals are still preserved (Fig. 8E).

The variation in size and shape of the zoned calcite crystals, presence of authigenic clay inclusions, growth of some crystals from micrite in the matrix, and presence of the zoned crystals in some spar patches indicates that these crystals are diagenetic products. They may have formed through dissolution and recrystallization of carbonate in the matrix, including fragmented pieces of charophytes and skeletal stromatolites. The crystals in the matrix are similar to zoned calcite fabrics in alpha-type calcretes (Wright 1988; Wright and Peeters 1989), although alpha fabrics tend to lack evidence of biogenic influences and were interpreted by Wright (1988) to represent an abiogenic end member of calcrete fabrics. The differences between the neomorphic calcite crystals in Unit 2 and alpha fabrics in calcretes, however, may simply reflect the same types of processes taking place in a palustrine context as opposed to a calcrete context.

Authigenic feldspar and clays (illite and kaolinite) are dispersed throughout the matrix of Unit 2. Some feldspar crystals show evidence of partial dissolution (Fig. 8F), but the timing of dissolution is not known. Clay minerals are also found randomly in the matrix and wrapped around some tubules (Fig. 8C, G). It is not always clear if these clays were deposited as sediment or are authigenic. Clays have not, however, been found as inclusions in charophytes or in any of the skeletal stromatolites.

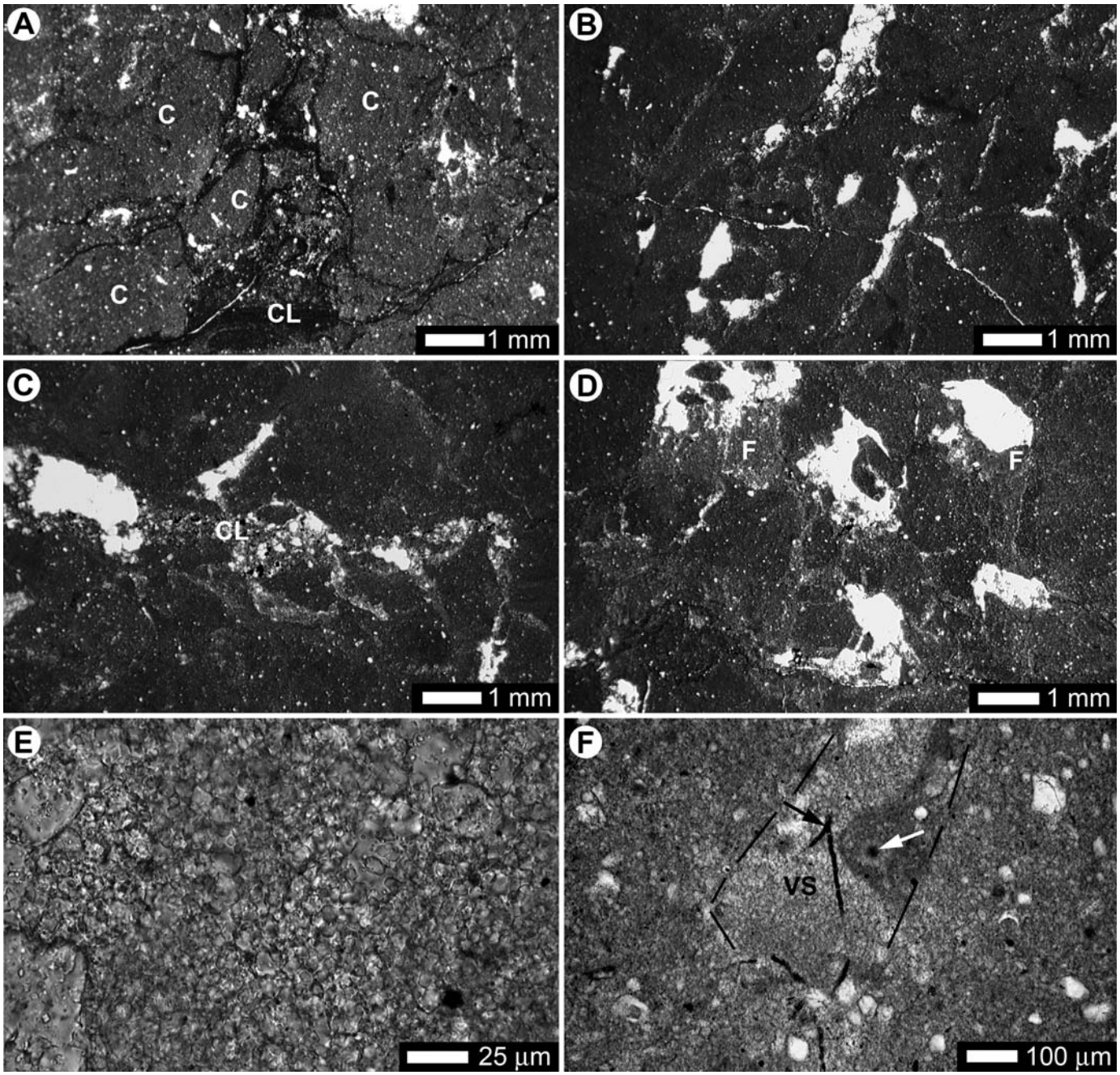

FIG. 6.—Thin-section photomicrographs of subaerial exposure and pedogenesis features in Unit 2. **A)** Matrix brecciation. Clasts (C) separated by cavities filled with clay-rich micrite and laminated clays (CL). **B)** Subvertical sinuous rootlets filled by micrite–clay mixtures and coarse calcite spar. **C)** Brecciated root trace partly filled by illite and kaolinite clays (CL) mixed with micrite. **D)** Fractured root traces partly filled by clay–micrite mixtures and vadose silt (F). Remaining space is filled by coarse calcite spar. **E)** Vadose silt. **F)** Rootlet (black outline) lined by micritic cutan with spherulite (white arrow) and filled with vadose silt (VS) that contains a branching segmented fungal hyphae or root hair (black arrow).

→

Fig. 7. Pedogenic features in Unit 2. A and C–E = thin-section photomicrographs; B and F–H = SEM photomicrographs. **A)** Irregular rootlet lined by laminated micrite and laminated micrite–clay features (arrows). **B)** Polished and etched clay-micrite lining. Clay laminations (arrows) are well defined, but etching removed most micrite, leaving epoxy. **C)** Rootlet with micrite–clay linings on walls (arrows) that spalled off at bottom right. Rootlet is filled by mix of vadose silt (VS) and coarse, inclusion-rich calcite rhombs (IC). **D)** Rootlet lined at base by discontinuous clay cutan (C) and filled by pockets of authigenic kaolinite (K), clay-micrite mixtures, and coarse inclusion-rich calcite (IC) crystals. **E)** Authigenic kaolinite booklets embedded in vadose silt (VS) in rootlet. **F)** Authigenic kaolinite booklets in rootlet arranged in vermiform patterns. **G)** Spar patch surrounded by transition zones (TZ) into surrounding micritic matrix. Etched sample. **H)** Concentrically zoned calcite in spar patch. Fractured sample.

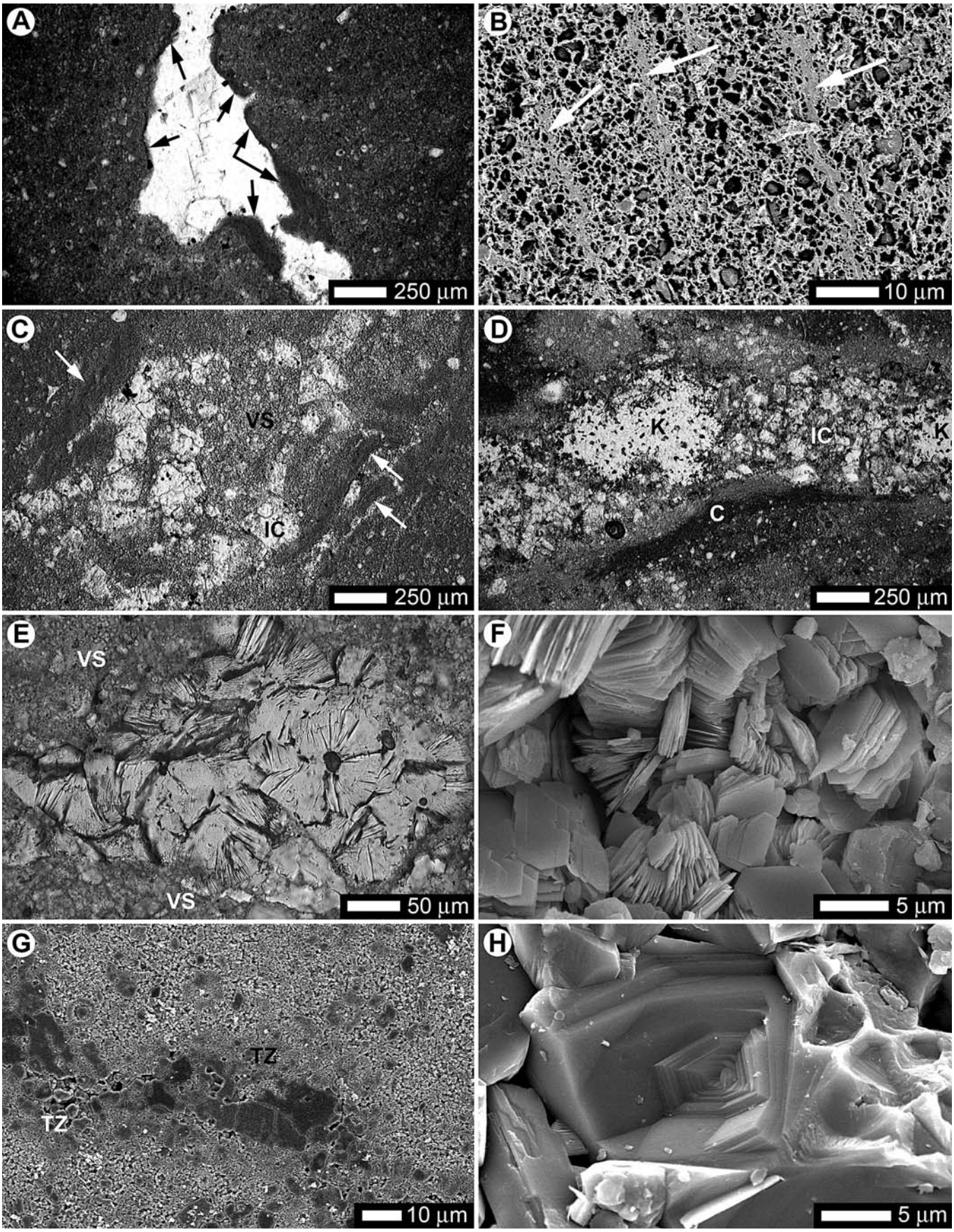
A
250 µm
B
10 µm
C
VS
IC
250 µm
D
K
IC
K
C
250 µm
E
VS
VS
50 µm
F
5 µm
G
TZ
TZ
10 µm
H
5 µm

Spherulites.—Spherulites (15–40 μm diameter) formed of irregular bladed calcite crystals that radiate from a sometimes hollow center are common throughout Unit 2 (Fig. 8H). Locally, they appear to be joined into composite structures. In contrast to the hollow spheres, which are abundant but randomly dispersed, the spherulites are, in some areas, closely associated with void systems and cutans (Figs. 6F, 8H). The origin of the spherulites is not clearly understood, but they may be pedogenic (e.g., Brewer 1964; Verrecchia et al. 1995).

Unit 3—The Marine-Incursion Deposit

Evidence of pedogenesis in Unit 3 includes small rhizocretions, poorly preserved root traces, irregular fracture patterns, and irregular patterns of staining by organics, Fe-sulfides, and Fe-oxides. Unlike the marine deposits in Unit 1 and Unit 4, Unit 3 is characterized at the outcrop scale by an irregular nodular texture formed from the variable alteration of the limestone, such that areas of hard limestone are separated by friable, chalky areas of soft limestone (Fig. 2B, C). This is similar to the subaerial alteration of Pleistocene limestones on Barbados (James 1972), in which remnants of the host limestone float in an intensely altered matrix, and Palustrine Facies #6 of Freytet (1973), attributed to oscillation of the water table.

Rhizocretions, Root Traces, and Fractures.—Rhizocretions, root traces, and irregular fracture networks, in some cases associated with brecciation, are variably preserved in Unit 3. The rhizocretions, formed of concentric micritic laminae, have small diameters (~ 1 mm) with variably stained outer margins and contain amorphous organic material and vadose silt (Fig. 9A). Root traces and irregular fracture networks intersect each other and are partly filled with brecciated clasts of matrix material, calcitic vadose silt, mixtures of calcitic vadose silt with illite, books of authigenic kaolinite arranged in vermiform patterns, Fe-oxide pigments, gypsum, and coarse calcite spar (Fig. 9B–D). Fine (~ 10 μm diameter), orange-brown segmented sinuous tubules that resemble fungal hyphae or root hairs are preserved locally in these voids (Fig. 9E), and in rare cases can be traced for lengths that exceed 1 mm.

Staining Patterns and Clots.—Throughout Unit 3 there are irregular nodular and stringer-like patterns of red and black staining caused by Fe-oxides and related pigments, very finely crystalline Fe-sulfides, and organics. Nodular stain patterns in the matrix, up to ~ 2 cm in diameter, are characterized by irregular, sharply defined to diffuse margins and variably stained interiors (Fig. 9F). *Amphipora* and other fossil fragments are variably stained, like those at the top of Unit 1. As such, the staining is treated as a subaerial alteration feature, like the staining at the top of Unit 1.

EVOLUTION OF THE COASTAL-PLAIN SUCCESSION

Deposits in the Alexandra Formation at the top of RC#1 record the evolution of a dynamic coastal-plain environment concurrent with fluctuating sea level and the offshore development of RC#2. Periods of subaerial exposure, weathering, and pedogenesis alternated with periods of fresh-water to brackish-water deposition and marine deposition. The cumulative succession, ~ 50 cm thick, represents a Type I sequence boundary that separates the marine deposits of RC#1 (Unit 1) from marine deposits of RC#2 (Unit 4). Five stages (1–5) in its evolution are evident (Fig. 10).

Stage 1: Initiation of Coastal Plain

RC#1 formed the limestone substrate to the coastal plain after sea level fell ~ 17 m (Fig. 10 #1). Whereas the reef-margin facies, several kilometers away, contain vadose cements in 1–3 cm solution vugs (MacNeil and Jones in press), the peritidal deposits in the Alexandra Falls region were stained by weathering processes. Storms transported blackened intraclasts from the coastal plain to the outer ramp, where they became common constituents of storm beds in the basal part of RC#2 (MacNeil and Jones in press).

Stage 2: Deposition of Palustrine Carbonate

In the Alexandra Falls area, establishment of shallow, carbonate-rich marshlands on the weathered limestones at the top of Unit 1 led to deposition of palustrine carbonate (Fig. 10 #2). Blackened intraclasts and stained *Amphipora* fragments from the top of Unit 1 were incorporated into these deposits. Root traces, crack networks, complex crystal fabrics, and authigenic mineral growth attest to exposure of the marsh deposits and pedogenesis on a vegetated coastal plain in an intermediate to semiarid climate (cf. Platt and Wright 1992).

Stage 3: Deposition of Sediment from Marine Incursion

Deposition and weathering of the palustrine carbonate was terminated by the incursion of marine waters onto the coastal plain. Shallow lagoon sediments dominated by *Amphipora* and algae were deposited along with storm detritus that may have been derived from the reef situated on the outer ramp (Fig. 10 #3).

Stage 4: Subaerial Exposure and Pedogenesis

Following retreat of the shoreline, subaerial exposure, weathering, and pedogenesis of Unit 3 produced features similar to those found in Unit 2 (Fig. 10 #4). The presence of gypsum in cavities indicates percolation of saline waters through the unit. Periodic establishment of saline ponds on the coastal plain, or sea spray, which may travel several kilometers inland (e.g., James 1972), may have provided this water.

Stage 5: Transgression and Deposition of Peritidal Facies

Subaerial weathering and pedogenesis at the top of Unit 3 was terminated by permanent flooding of the coastal plain that established an inland peritidal region to RC#2 (Fig. 10 #5). These deposits form the upper part of the Alexandra Formation.

DISCUSSION

Features at the top of Unit 1 and in Unit 2 and Unit 3 (Table 1) are interpreted to collectively reflect events of subaerial exposure and pedogenesis that took place on the coastal plain after falling sea level

→

Fig. 8. Pedogenic-diagenetic features in Unit 2. A = Thin-section photomicrograph; B–H = SEM photomicrographs. **A)** Zoned spar crystal in matrix with tubule inclusions at outer edges (arrows). **B)** Spar crystal in matrix with growth zonations (Z) and matrix embayments (E), authigenic kaolinite inclusions (C), and matrix inclusions (M). Matrix inclusions presumably formed after diagenetic overgrowth of matrix embayments. **C)** Interlocking micrite (IM) and zoned microspar (MS) growing on surface of authigenic kaolinite booklet. **D)** Microspar overgrowths of micrite, trapping some micritic matrix as inclusions. **E)** Crystal with filament extending from its edge (arrow). It is not clear if the filament penetrated the crystal or the crystal grew around the filament. **F)** Partly dissolved authigenic feldspar (F). **G)** Tubule lined by clays. **H)** Spherulite surrounded by zoned (Z) spar. Irregular edges of the zoned spar against the spherulite suggest that it grew against the preexisting spherulite.

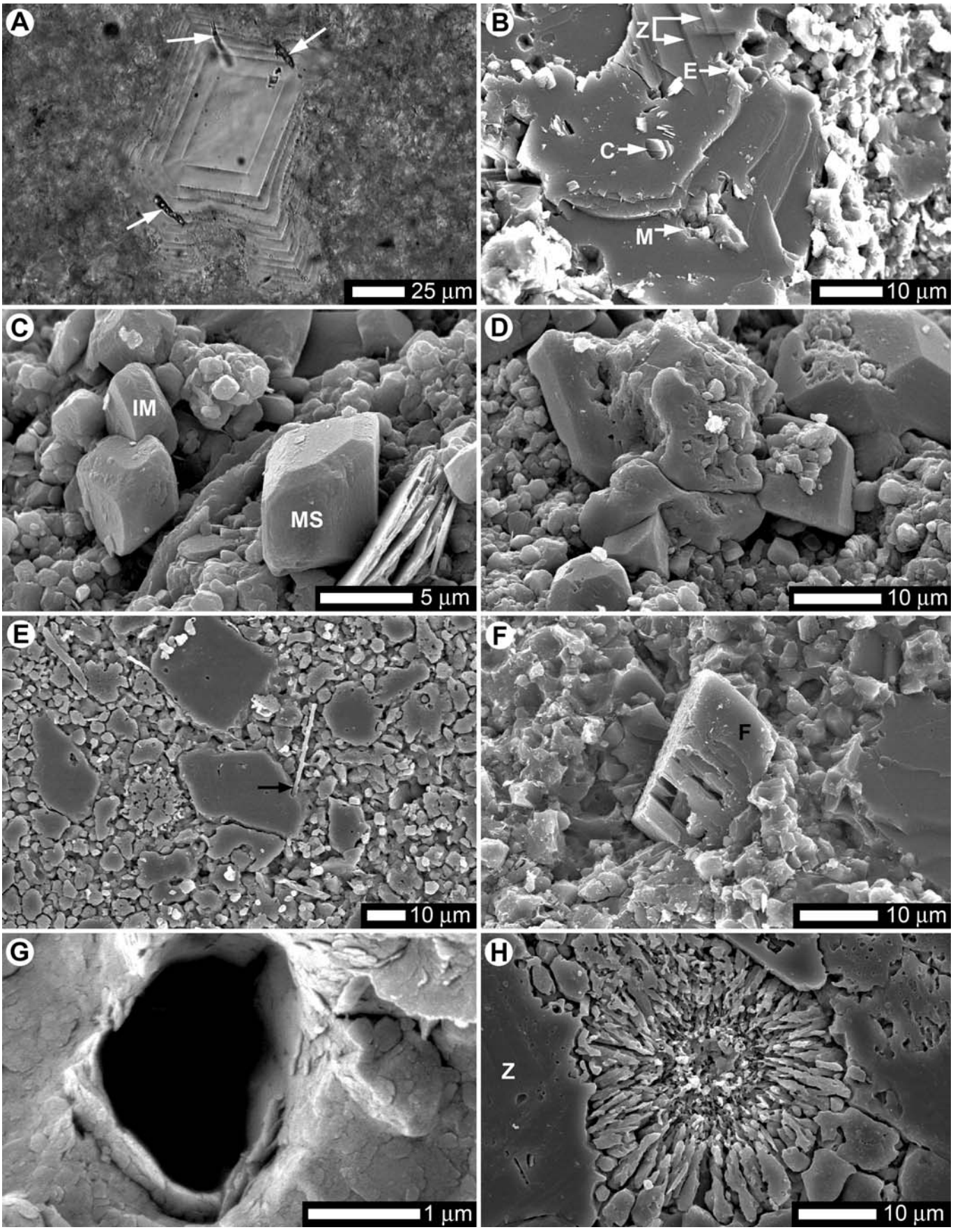
A
25 µm
B
Z
E
C
M
10 µm
C
IM
MS
5 µm
D
10 µm
E
10 µm
F
F
10 µm
G
1 µm
H
Z
10 µm

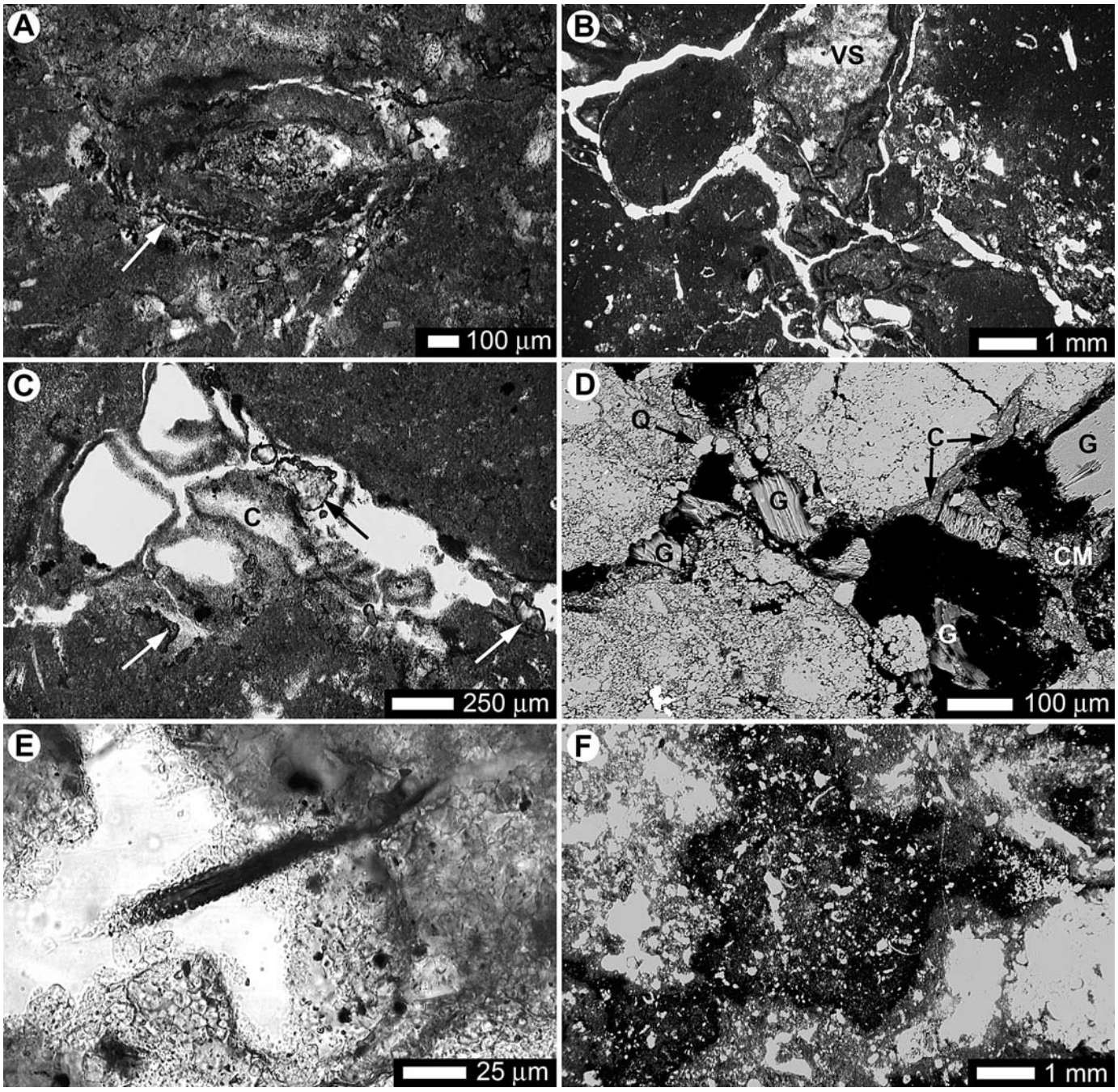

FIG. 9.—Pedogenic features in Unit 3. A–C, E, and F = thin section photomicrographs; D = BSE image. **A)** Rhizocretion with micritic laminae and partly stained outer edge (arrow). Central part of rhizocretion partly filled with organics and micrite. **B)** Complex crack and root-trace network. Root trace filled with vadose silt (VS). Crack network filled with mix of clays, micrite, gypsum, and spar. **C)** Close-up of irregular clay-micrite (C) material filling part of crack network. Clays are a mix of illite and kaolinite. Gypsum (arrows) partly filled remaining space. **D)** Crack network partly lined and filled with clays (C) and filled with clay–micrite mixtures (CM), quartz (Q), and gypsum (G). Black = pore space. **E)** Orange-brown hollow, segmented tube in crack network. **F)** Nodular stain pattern in matrix defined by concentrated halo of black staining and lesser staining of interior.

exposed the top of Reef Complex #1. Features of the palustrine deposit are comparable with those documented from other palustrine deposits and calcretes (e.g., Brewer 1964; Freytet 1973; Bal 1975; Freytet and Plaziat 1982; Wieder and Yaalon 1974, 1982; Braithwaite 1983; Esteban and Klappa 1983; Platt 1989; Tandon and Friend 1989; Platt and Wright 1992; Dunagan and Driese 1999; Alonso-Zarza 2003). Features in Unit 3 are comparable with alteration features found in limestones at subaerial unconformities and below calcrete profiles (e.g., James 1972; Driese et al. 1994).

Although it is reasonable to assume that subaerial alteration of Unit 2 and Unit 3 reached depths below their bases and may have imparted pedogenic or diagenetic features onto the underlying deposits, there is limited evidence for this possibility having taken place. Blackened intraclasts in Unit 2, derived from the top of Unit 1, indicate that

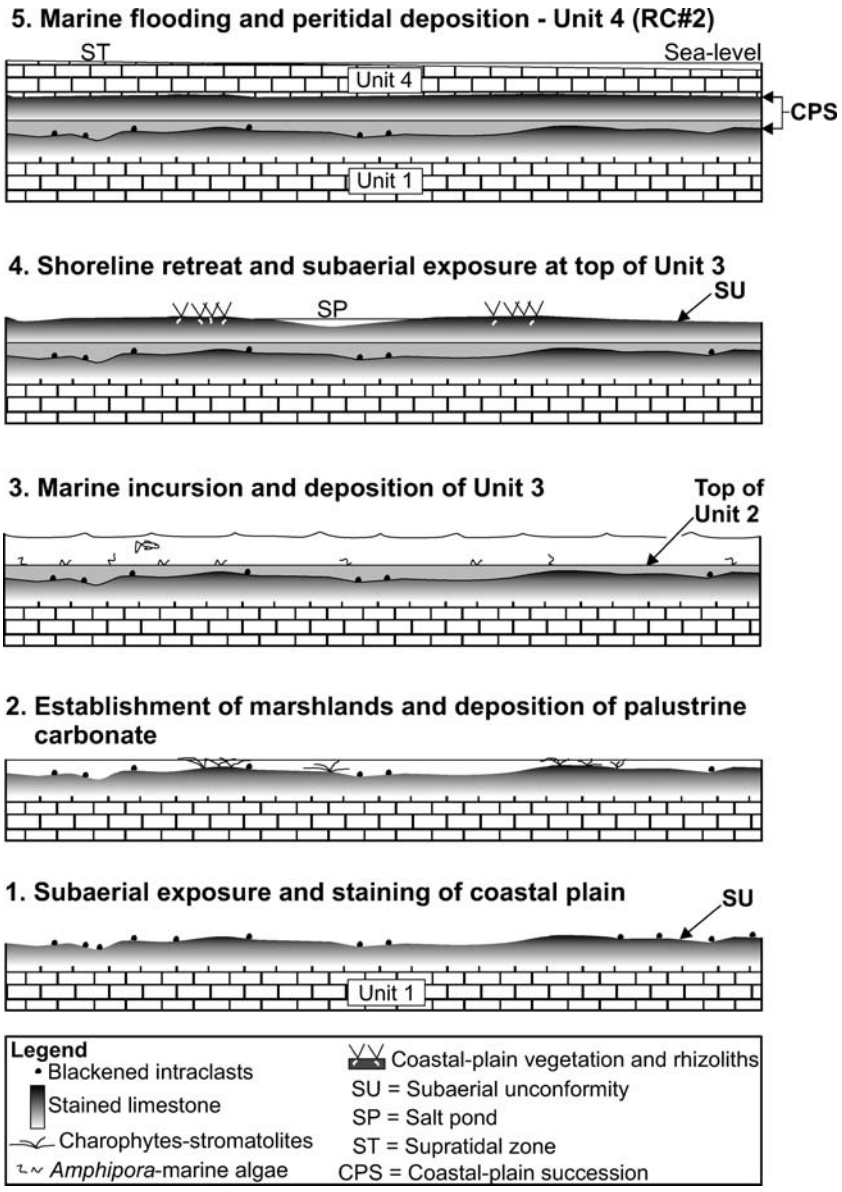

FIG. 10.—Evolution of coastal-plain succession in Alexandra Formation after sea-level fall terminated development of RC#1 and exposed its top. Stages 1–4 took place while RC#2 developed on outer ramp. Final stratigraphic succession is illustrated in #5. Not to scale.

TABLE 1.—*Features indicative of subaerial exposure and pedogenesis found in coastal-plain succession at top of RC#1 in Alexandra Formation along Hay River.*

Unit 1	Unit 2	Unit 3
Blackened/reddened Fe-staining	Nodular texture	Chalky differentiation of outcrop
	Crack networks	Crack networks
	Root traces	Root traces
	Brecciated root traces	Rhizocretions
	Vadose silt	Vadose silt
	Authigenic kaolinite, feldspar, illite	Authigenic kaolinite, illite
	Spar patches with diffusive margins	Fracture-filling gypsum
	Clay cutans and micrite and micrite-clay cutans or biofilms	Blackened/reddened Fe-staining
	Neomorphic calcite	
	Neomorphic calcite with siliciclastic inclusions, matrix embayments	
	Spherulites	

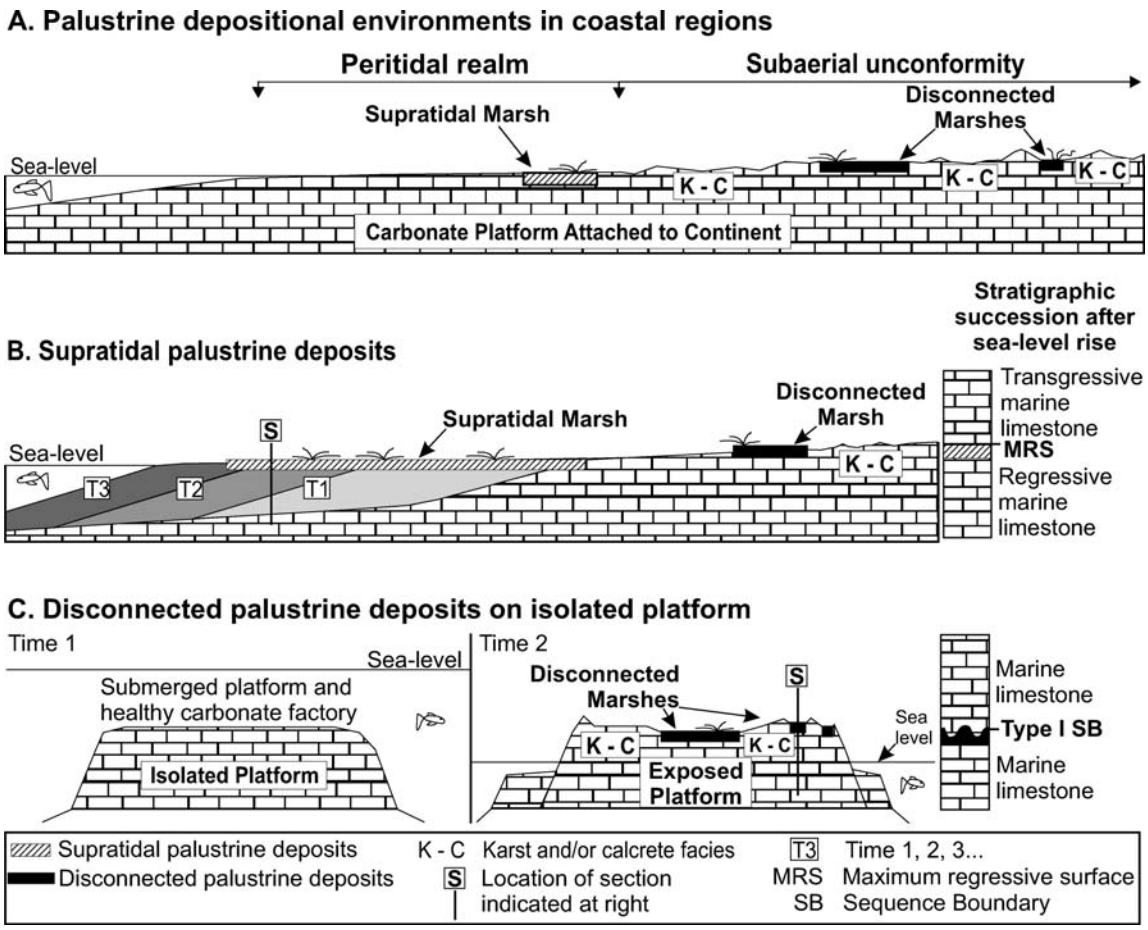

FIG. 11.—Context of palustrine deposits in marine coastal environments (not to scale). **A)** Spectrum of palustrine deposits in coastal regions defined by supratidal and disconnected end members. **B)** Supratidal deposits capping progradational, normal regressive system. Note that supratidal palustrine deposits connect landwards with subaerial unconformity, which may include disconnected palustrine deposits. Sea-level rise and transgression would result in a regressive–transgressive marine limestone succession (column at right), divided by supratidal palustrine deposits. Top of supratidal palustrine deposits marks maximum regressive surface. **C)** Disconnected palustrine deposits on isolated oceanic platform. Carbonate sediment deposited when platform is submerged (Time 1) will be subaerially exposed upon relative sea-level fall of sufficient magnitude (Time 2). The subaerial unconformity may be marked by karst, calcrete, and/or disconnected palustrine deposits. Subsequent relative sea-level rise may deposit new sequence of marine limestone. The two marine limestone sequences (column at right) are separated by a Type I sequence boundary marked by disconnected palustrine deposits.

staining at the top of Unit 1 took place before Unit 2 was deposited and is distinct from the staining of Unit 3. Likewise, ripped-up lithoclasts of Unit 2 with zoned neomorphic calcite in Unit 3 indicate that these features developed prior to deposition of Unit 3. The root traces in Unit 2 probably formed close to the surface of that unit, rather than at depth from the top of Unit 3, because they are delicate forms (e.g., $\leq$ 2 mm diameter) and robust (e.g., $>$ 2 mm diameter), deeply penetrative root traces are not present in Unit 3. The authigenic kaolinite that fills some voids in Unit 2 may be genetically related to the kaolinite in Unit 3, but the absence of gypsum in the voids of Unit 2, which is common in the voids of Unit 3, suggests that downward percolation of waters was minimal and that the kaolinite in each unit is probably distinct. Neither authigenic kaolinite nor gypsum have been found in Unit 1, Unit 4, or any other part of the Alexandra Formation.

The coastal-plain succession has regional stratigraphic significance because it marks the termination of RC#1 and separates RC#1 from RC#2. The amount of time represented by the succession, however, is unknown because of the lack of precise biostratigraphic controls due to the absence of age-diagnostic fossils (McLean and Klapper 1998) and deposits suitable for absolute age dating. Comparison of the magnitude of sea-level fall ($\sim$ 17 m) to sea-level fluctuations (third–fifth order cycles) for greenhouse and transitional climates, which characterized the Late Devonian (e.g., Copper 2002), however, suggests that the boundary between RC#1 and RC#2 is a relatively high-frequency boundary, with even higher-frequency superimposed shoreline shifts. The latter is indicated by the deposition of Unit 3, which probably took place at the top of the lowstand systems tract in which RC#2 was developing. Given the magnitude of sea-level fall, it seems reasonable that the coastal-plain succession represents a fourth-order sequence boundary with a hiatus of 0.1–1 Myr. The higher-frequency deposits that form Unit 3 may be of 0.01–0.1 Myr duration (cf. Tucker et al. 1993; Lehrmann and Goldhammer 1999). The amount of time represented by Unit 2 is unknown.

The significance of palustrine deposits, which can cover thousands of square kilometers in coastal regions (Platt and Wright 1992), to the sequence stratigraphic analysis of marine limestone successions, has yet to be fully realized. There are two end-member contexts in marine coastal environments where palustrine deposits can be found (Fig. 11A), with each conveying different stratigraphic implications.

At one end of the spectrum (where climate permits) are fresh- to brackish-water marshes situated in supratidal environments, subject to periodic flooding by seawater during spring tides and storm events (e.g.,

TABLE 2.—*Criteria for recognition and distinction of supratidal palustrine deposits, disconnected palustrine deposits, karst, and pedogenic calcrete.*

	Supratidal Palustrine Deposits	Disconnected Palustrine Deposits	Karst	Pedogenic Calcrete
Sedimentary setting	Marshes in supratidal realm	Marshes on subaerially exposed platform	Subaerially exposed platform	Subaerially exposed platform
Sedimentary nature	Fresh-brackish water deposits; periodic exposure and pedogenesis	Fresh-brackish water deposits; periodic exposure and pedogenesis	Subaerial erosion of limestone by meteoric diagenesis	Erosion of limestone substrate and pedogenesis
Distinctive features	Sediment-binding stromatolites dominant; fenestral porosity; skeletal stromatolites	Charophytes and skeletal stromatolites (e.g., *Rivularia haematites*) abundant	Sink holes, caverns, speleothems, solution vugs, phytokarst	Nodular, platy, laminar, chalky pedogenic horizons; possibly colour (e.g., red, green)
	Contain storm-derived marine sediment and may appear to be cyclical marine deposits	No marine sediment. May contain peat and occur with lacustrine facies, karst, and/or calcrete		Do not contain primary charophyte-skeletal stromatolite associations
Important attributes	Rhizoliths, desiccation cracks, brecciation, circumgranular cracks, blackened intraclasts, vadose silt, cutans, spar patches, Microcodium, neomorphic calcite, authigenic clays and feldspar, spherulites	Rhizoliths, desiccation cracks, brecciation, circumgranular cracks, blackened intraclasts, vadose silt, cutans, spar patches, *Microcodium*, neomorphic calcite, authigenic clays and feldspar, spherulites	Rhizoliths, collapse breccias, blackened intraclasts, terra rossa, vadose silt and cements	Rhizoliths, desiccation cracks, brecciation, circumgranular cracks, blackened intraclasts, vadose silt, cutans, spar patches, *Microcodium*, calcite tubules, authigenic clays and feldspar, alpha fabrics, lichen, pisoids, spherulites
Indicates subaerial unconformity	NO	YES	YES	YES

Lists compiled from features identified in this paper and in Monty and Hardie (1976), Shinn (1983), Esteban and Klappa (1983), and Platt and Wright (1992).

Monty and Hardie 1976; Shinn 1983). In this context, the marshes represent marginal depositional systems to the surrounding marine system, thereby acting as a connect, or transition zone, between conformable deposits in the marine realm and the adjacent subaerial unconformity (Fig. 11A). Deposits in these marshes have distinct sedimentary features (Table 2) that unequivocally point to their location in the peritidal realm (Monty and Hardie 1976; Shinn 1983). Because peritidal facies associations track sea-level fluctuations, the stratigraphic implications of these deposits are well known; supratidal palustrine deposits can be predicted to cap normal regressive peritidal systems (Fig. 11B) or be found at the bases of transgressive peritidal systems (Monty and Hardie 1976; Wright 1985). The top of supratidal palustrine deposits in normal regressive deposits indicates therefore the point of maximum regression and will be overlain by transgressive deposits if sea-level rises (Fig. 11B), or by a sequence boundary if relative sea level falls. In contrast, supratidal palustrine deposits at the base of a transgressive peritidal system are subject to intense erosion as the tidal flat retrogrades and are not likely to be preserved (Wright 1985).

At the opposite end of the spectrum are palustrine deposits that form in marshes that are not associated with the peritidal realm but are juxtaposed onto subaerial unconformities (Fig. 11A). These deposits may be directly associated with karst and/or calcrete (e.g., Monty and Hardie 1976; Esteban and Klappa 1983; Platt and Wright 1992). Described herein as "disconnected" palustrine deposits, the marshes in which these deposits originate are isolated from direct marine influence and form part of the exposed landscape (Fig. 11A–C). As such, disconnected palustrine deposits are distinguishable from supratidal palustrine deposits (Table 2; cf. Monty and Hardie 1976) and should be considered a sedimentary component of subaerial unconformities and sequence boundaries. Modern examples of disconnected palustrine deposits include marshes in the interior eastern half of Andros Island in the Bahamas (e.g., Monty and Hardie 1976) and marshes in the interiors of the Cayman Islands (personal observations of the authors). Palustrine deposits in the Florida Everglades (e.g., Platt and Wright 1992) cover a continuum from those that are disconnected from marine influence to those that are deposited proximal to the mangrove swamps and salt marshes. In all of these examples, the palustrine deposits are characterized by very thin (< 1 m) deposits surrounded by elevated (centimeter to decimeter scale) areas with concurrently developing karst and/or calcrete (cf. Monty and Hardie 1976; Platt and Wright 1992). After a relative sea-level rise that leads to permanent marine flooding, these deposits, in addition to the karst and/or calcrete, mark the sequence boundary (Fig. 11C). They are distinct from overlying transgressive deposits because (1) they are not conformable with these deposits, as shown by their inherent evidence of exposure and pedogenesis (cf. Freytet 1973; Freytet and Plaziat 1982; Esteban and Klappa 1983; Platt and Wright 1992; Dunagan and Driese 1999; Alonso-Zarza 2003), (2) they were deposited, and altered, concurrently with surrounding calcrete and/or karst, which constitute the other criteria for identifying the sequence boundary (cf. James 1972; Esteban and Klappa 1983; Sarg 1988; Handford and Loucks 1993; Hunt and Tucker 1993), and (3) transgression in carbonate systems is usually characterized by a lag between the initial flooding event and subsequent onset of deposition (e.g., mangrove peat), during which physical and biological erosion takes place (Enos 1977; Harris 1979; Hardie and Shinn 1986; Desrochers and James 1988; Jones and Hunter 1989; Jones and Desrochers 1992; Gischler 2003). As such, the base of the transgressive depositional succession is the erosional surface (e.g., a ravinement surface) that is found at the top of the palustrine deposit (cf. Jones and Desrochers 1992).

The importance of revising the criteria for recognizing subaerial unconformities and defining sequence boundaries in marine limestone successions (Table 2, Fig. 11) is exemplified in the Alexandra Formation, where karst features and calcrete profiles are not found at the boundary between RC#1 and RC#2. In this case, the coastal-plain deposits in Unit 2 originated in marshlands situated on the subaerial unconformity developed at the top of Unit 1, which is notable only for its stained

appearance. The sedimentology of the marshlands indicates that they were isolated from the marine realm in which RC#2 was developing, and were not part of a supratidal depositional environment. Given that overlying Unit 3 also includes evidence of subaerial exposure and pedogenesis, the hiatus at its top is identified as the physical surface that defines the top of the coastal-plain succession and separates the depositional sequence of RC#1 from that of RC#2. Deposition of Unit 3 was probably a prelude to the more permanent flooding that deposited Unit 4, as part of RC#2.

Recognition of ancient disconnected palustrine deposits is important because of their stratigraphic implications. Successful recognition of these deposits, however, may be difficult because (1) root traces may be mistaken for animal burrows, (2) the deposits may be structureless (Wright 1985) or nodular, which is not solely diagnostic, (3) fossil content may be sparse and the ecology of many ancient microfossils remains poorly understood, and (4) calcrete and/or karst features, which would suggest a terrestrial origin to the deposit, may not be co-developed, as seen in the Alexandra Formation. Wright (1985) noted that failure to recognize these deposits, when they do occur, must partly explain their limited record. Palustrine deposits may also be easily mistaken for calcrete, given that a number of features are common to both types of deposits (Freytet and Plaziat 1982; Esteban and Klappa 1983; Alonso-Zarza 2003). The association of charophytes with *Rivularia* skeletal stromatolites, therefore, is an important depositional feature that should aid in the recognition of ancient palustrine deposits. In modern marshlands, calcareous streams, and rice fields, charophyte–microbe, and in particular, charophyte–*Rivularia* associations, are well documented (e.g., Freytet and Plaziat 1982; Whitton 1987). Monty (1976), for example, noted that colonies of *Rivularia haematites* are commonly found in the splash zones of lakes, which is where palustrine deposits would be accumulating. As such, inclusion of charophyte–skeletal stromatolite associations with sedimentary and pedogenic features (Table 2) provides an enhanced set of criteria for the identification of ancient, disconnected palustrine deposits, and distinction of these deposits from supratidal palustrine deposits and calcrete. Although a few examples of calcified *Rivularia* are known from marine environments (e.g., Golubic and Campbell 1981), these precipitates are distinct from freshwater *Rivularia* precipitates and are likely to be associated with marine biota, thereby allowing distinction from those in palustrine deposits.

CONCLUSIONS

The unconformable nature of the coastal-plain succession in the Alexandra Formation is deceptive because it lacks karst features and calcrete profiles. The palustrine deposits, however, which are distinct from all other facies in the Alexandra Formation, provide unequivocal evidence that a fresh- to brackish-water environment, disconnected from the marine realm, existed at this stratigraphic level. Conclusions from this study include:

1. RC#2 was fringed by a coastal plain developed at the top of RC#1, on which a series of unconformable deposits were deposited in an intermediate to semiarid climate. The most distinct were the palustrine deposits, and the succession represents a Type I sequence boundary.
2. The sequence boundary probably represents a hiatus of 0.1–1.0 Myr, with higher-frequency sea-level fluctuations superimposed.
3. Disconnected palustrine deposits should be considered important criteria for recognizing subaerial unconformities in marine limestone successions.
4. Disconnected palustrine deposits, calcrete profiles, and/or karst are the criteria for defining sequence boundaries in successions of marine limestones.
5. Ancient palustrine deposits can be recognized through a set of depositional and pedogenic criteria that include charophyte–skeletal stromatolite associations. This association distinguishes palustrine deposits from calcrete, which share a number of the same pedogenic features.

ACKNOWLEDGMENTS

The authors are grateful for the financial support of this project by the Canadian Circumpolar Institute at the University of Alberta, Northern Science Training Program of the Department of Indian Affairs and Northern Development, the American Association of Petroleum Geologists Grant-in-Aid Foundation (to MacNeil), Natural Sciences and Engineering Research Council of Canada (PGSB to MacNeil and grant A6090 to Jones), and the C.R. Stelck Chair of Petroleum Geology held by B. Jones. We are also indebted to Don Resultay and Mark Labbe, who prepared the thin sections, and George Braybook who operated the SEM. All fieldwork was conducted with permits granted by the Aurora Research Institute of the Northwest Territories. Drs. S. Driese, G.J. Retallack, and B. Wilkinson are thanked for reviewing an earlier draft of this manuscript and providing constructive comments that led to its enhancement.

REFERENCES

Alonso-Zarza, A.M., 2003, Palaeoenvironmental significance of palustrine carbonates and calcretes in the geological record: Earth-Science Reviews, v. 60, p. 261–298.

Bal, L., 1975, Carbonate in soil: a theoretical consideration on, and proposal for its fabric analysis. 1. Crystic, calcic and fibrous plasmic fabric: Netherlands Journal of Agricultural Science, v. 23, p. 18–35.

Bellow, J.M., 1993. The sedimentology and stratigraphy of the Alexandra Formation, Hay River region, Northwest Territories [unpublished M.Sc. Thesis]: Edmonton, University of Alberta, 78 p.

Belyea, H.R., and McLaren, D.J., 1962. Upper Devonian Formations, southern part of Northwest Alberta: Geological Survey of Canada, Paper 61-29, 72 p.

Bertrand-Sarfati, J., 1976, An attempt to classify Late Precambrian stromatolite microstructures, *in* Walter, M.R., ed., Stromatolites: Amsterdam, Elsevier, Developments in Sedimentology 20, p. 251–259.

Braithwaite, C.J.R., 1983, Calcrete and other soils in Quaternary limestones: structures, processes and applications: Geological Society of London, Journal, v. 140, p. 351–363.

Brewer, R., 1964. Fabric and Mineral Analysis of Soils: New York, John Wiley & Sons, 470 p.

Caudwell, C., Lang, J., and Pascal, A., 2001, Lamination of swampy–rivulets *Rivularia haematites* stromatolites in a temperate climate: Sedimentary Geology, v. 143, p. 125–147.

Copper, P., 2002, Reef development at the Frasnian/Famennian mass extinction boundary: Palaeogeography, Palaeoclimatology, Palaeoecology, v. 181, p. 27–65.

Desrochers, A., and James, N.P., 1988, Early Paleozoic surface and subsurface paleokarst: Middle Ordovician Carbonates, Mingan Islands, Quebec, *in* James, N.P., and Choquette, P.W., eds., Paleokarst: Berlin, Springer-Verlag, p. 183–210.

Drees, L.R., and Wilding, L.P., 1987, Micromorphic record and interpretations of carbonate forms in the rolling plains of Texas: Geoderma, v. 40, p. 157–175.

Driese, S.G., Srinivasan, K., Mora, C.I., and Stapor, F.W., 1994, Paleoweathering of Mississippian Monteagle Limestone preceding development of a lower Chesterian transgressive systems tract and sequence boundary, middle Tennessee and northern Alabama: Geological Society of America, Bulletin, v. 106, p. 866–878.

Dunagan, S.P., and Driese, S.G., 1999, Control of terrestrial stabilization on Late Devonian palustrine carbonate deposition: Catskill Magnafacies, New York, USA: Journal of Sedimentary Research, v. 69, p. 772–783.

Dunham, R.J., 1969, Early vadose silt in Townsend mound (reef), New Mexico, *in* Friedman, G.M., ed., Depositional Environments in Carbonate Rocks: SEPM, Special Publication 14, p. 139–181.

Enos, P., 1977, Holocene sediment accumulation of the south Florida shelf margin, *in* Enos, P., and Perkins, R.D., eds., Quaternary sedimentation in south Florida: Geological Society of America, Memoir 147, p. 1–130.

Esteban, M., and Klappa, C.F., 1983, Subaerial exposure environment, *in* Scholle, P.A., Bebout, D.G., and Moore, C.H., eds., Carbonate Depositional Environments: American Association of Petroleum Geologists, Memoir 33, p. 1–54.

Folk, R.L., 1959, Practical petrographic classification of limestones: American Association of Petroleum Geologists, Bulletin, v. 43, p. 1–38.

Freytet, P., 1973, Petrography and paleo-environment of continental carbonate deposits with particular reference to the Upper Cretaceous and Lower Eocene of Languedoc (southern France): Sedimentary Geology, v. 10, p. 25–60.

Freytet, P., and Plaziat, J.-C., 1982, Continental carbonate sedimentation and pedogenesis—Late Cretaceous and early Tertiary of southern France, *in* Purser, B.H., ed., Contributions to Sedimentology 12: Stuttgart, E. Schweizerbart'che Verlagsbuchhandlung (Nägele u. Obermiller), 213 p.

Freytet, P., and Plet, A., 1996, Modern freshwater microbial carbonates: The *Phormidium* stromatolites (tufa-travertine) of southeastern Burgundy (Paris Basin, France): Facies, v. 34, p. 219–238.

Freytet, P., and Verrecchia, E.P., 1998, Freshwater organisms that build stromatolites: a synopsis of biocrystallization by prokaryotic and eukaryotic algae: Sedimentology, v. 45, p. 535–563.

Gischler, E., 2003, Holocene lagoonal development in the isolated carbonate platforms off Belize: Sedimentary Geology, v. 159, p. 113–132.

Golubic, S., and Campbell, S.E., 1981, Biogenically formed aragonite concretions in marine *Rivularia*, *in* Monty, C., ed., Phanerozoic Stromatolites: Berlin, Springer, p. 209–229.

Golubic, A., Seong-Joo, L., and Browne, K.M., 2000, Cyanobacteria: architects of sedimentary structures, *in* Riding, R.E., and Awramik, S.M., eds., Microbial Sediments: Berlin, Springer-Verlag, p. 57–67.

Guo, L., and Riding, R., 1992, Aragonitic laminae in hot water travertine crusts, Rapolano Terme, Italy: Sedimentology, v. 39, p. 1067–1079.

Handford, C.R., and Loucks, R.G., 1993, Carbonate depositional sequences and systems tracts—Responses of carbonate platforms to relative sea-level changes, *in* Loucks, R.G., and Sarg, J.F., eds., Carbonate Sequence Stratigraphy: Recent Developments and Applications: American Association of Petroleum Geologists, Memoir 57, p. 3–42.

Hardie, L.A., 1987, Dolomitization: a critical view of some current views: Journal of Sedimentary Petrology, v. 57, p. 166–183.

Hardie, L.A., and Shinn, E.A., 1986, Carbonate depositional environments: modern and ancient. Part 3: Tidal Flats: Colorado School of Mines, Quarterly, v. 81, 74 p.

Harris, P.M., 1979. Facies anatomy and diagenesis of a Bahamian ooid shoal: Sedimenta 7, Comparative Sedimentology Laboratory: University of Miami, 163 p.

Hunt, D., and Tucker, M.E., 1993, Sequence stratigraphy of carbonate shelves with an example from the mid-Cretaceous (Urogonian) of southeast France, *in* Posamentier, H.W., Summerhayes, C.P., Haq, B.U., and Allen, G.P., eds., Sequence Stratigraphy and Facies Associations: International Association of Sedimentologists, Special Publication 18, p. 307–341.

James, N.P., 1972, Holocene and Pleistocene calcareous crust (caliche) profiles: criteria for subaerial exposure: Journal of Sedimentary Petrology, v. 42, p. 817–836.

Jamieson, E.R., 1967. The Alexandra reef-complex (Frasnian), Hay River area, NWT, Canada: stratigraphy, sedimentology, and palaeoecology [unpublished Ph.D. Thesis]: Reading, University of Reading, 220 p.

Jones, B., 1992, Construction of spar calcite crystals around spores: Journal of Sedimentary Petrology, v. 62, p. 1054–1057.

Jones, B., and Desrochers, A., 1992, Shallow Platform Carbonates, *in* Walker, R.G., and James, N.P., eds., Facies Models—Response to Sea Level Change: Geological Association of Canada, p. 277–302.

Jones, B., and Hunter, I.G., 1989, The Oligocene–Miocene Bluff Formation on Grand Cayman: Caribbean Journal of Science, v. 25, p. 71–85.

Jones, B., and Kahle, C.F., 1995, Origin of endogenetic micrite in karst terrains: a case study from the Cayman Islands: Journal of Sedimentary Research, v. 65, p. 283–293.

Klapper, G., and Lane, H.R., 1985, Upper Devonian (Frasnian) conodonts of the *Polygnathus* biofacies, N.W.T., Canada: Journal of Paleontology, v. 44, p. 801–815.

Lehrmann, D.J., and Goldhammer, R.K., 1999, Secular variation in parasequence and facies stacking patterns of platform carbonates: A guide to application of stacking-patterns analysis in strata of diverse ages and settings, *in* Harries, P.M., Saller, A.H., and Simo, J.A., eds., Advances in Carbonate Sequence Stratigraphy: Application to Reservoirs, Outcrops, and Models: SEPM, Special Publication 63, p. 187–226.

MacNeil, A.J., and Jones, B., in press, Sequence stratigraphy of a Late Devonian ramp-situated reef system in the Western Canada Sedimentary Basin: Dynamic responses to sea-level change and regressive reef development: Sedimentology.

McLean, R.A., and Klapper, G., 1998, Biostratigraphy of Frasnian (Upper Devonian) strata in western Canada, based on conodonts and rugose corals: Bulletin of Canadian Petroleum Geology, v. 46, p. 515–563.

Monty, C.L.V., 1976, The origin and development of cryptalgal fabrics, *in* Walter, M.R., ed., Stromatolites: Amsterdam, Elsevier, Developments in Sedimentology 20, p. 193–249.

Monty, C.L.V., and Hardie, L.A., 1976, The geological significance of the freshwater blue-green algal calcareous marsh, *in* Walter, M.R., ed., Stromatolites: Amsterdam, Elsevier, Developments in Sedimentology 20, p. 447–477.

Pentecost, A., 1978, Blue-green algae and freshwater carbonate deposits: Royal Society (London), Proceedings, v. 200 (Series B), p. 43–61.

Pentecost, A., 1987, Growth and calcification of the freshwater cyanobacterium *Rivularia haematites*: Royal Society (London), Proceedings, v. 232 (Series B), p. 125–136.

Pentecost, A., and Edwards, G.M., 2003, Raman spectroscopy and light microscopy of a modern and sub-fossil microstromatolite: *Rivularia haematites* (cyanobacteria, Nostocales): International Journal of Astrobiology, v. 1, p. 357–363.

Platt, N.H., 1989, Lacustrine carbonates and pedogenesis: sedimentology and origin of palustrine deposits from the Early Cretaceous Rupelo Formation, W. Cameros Basin, N. Spain: Sedimentology, v. 36, p. 665–684.

Platt, N.H., and Wright, V.P., 1992, Palustrine carbonates and the Florida Everglades: Towards an exposure index for the fresh-water environment: Journal of Sedimentary Petrology, v. 62, p. 1058–1071.

Posamentier, H.W., and Vail, P.R., 1988, Eustatic controls on clastic deposition I—sequence and systems tract models, *in* Wilgus, C.K., Hastings, B.S., Kendall, C.G.St.C., Posamentier, H.W., Ross, C.A., and Van Wagoner, J.C., eds., Sea-Level Changes: An Integrated Approach: SEPM, Special Publication 42, p. 109–124.

Pratt, B.R., 1984, *Epiphyton* and *Renalcis*—Diagenetic microfossils from calcification of coccoid blue-green algae: Journal of Sedimentary Petrology, v. 54, p. 948–971.

Purvis, K., and Wright, V.P., 1991, Calcretes related to phreatophytic vegetation from the Middle Triassic Otter Sandstone of south west England: Sedimentology, v. 38, p. 539–551.

Riding, R., 1991, Classification of microbial carbonates, *in* Riding, R., ed., Calcareous Algae and Stromatolites: Berlin, Springer-Verlag, p. 21–51.

Riding, R., 2000, Microbial carbonates: the geological record of calcified bacterial–algal mats and biofilms: Sedimentology, v. 47 (suppl. 1), p. 179–214.

Sarg, J.F., 1988, Carbonate sequence stratigraphy, *in* Wilgus, C.K., Hastings, B.S., Kendall, C.G.St.C., Posamentier, H.W., Ross, C.A., and Van Wagoner, J.C., eds., Sea-Level Changes: An Integrated Approach: SEPM, Special Publication 42, p. 155–182.

Sehgal, J.L., and Stoops, G., 1972, Pedogenic calcite accumulation in arid and semi-arid regions of the Indo-Gangetic alluvial plain of Erstwhile Punjab (India) —their morphology and origin: Geoderma, v. 8, p. 59–72.

Shinn, E.A., 1983, Tidal flat environment, *in* Scholle, P.A., Bebout, D.G., and Moore, C.H., eds., Carbonate Depositional Environments: American Association of Petroleum Geologists, Memoir 33, p. 171–210.

Shinn, E.A., and Lidz, B.H., 1988, Blackened limestone pebbles: fire at subaerial unconformities, *in* James, N.P., and Choquette, P.W., eds., Paleokarst: Berlin, Springer-Verlag, p. 117–131.

Strasser, A., 1984, Black-pebble occurrence and genesis in Holocene carbonate sediments (Florida Keys, Bahamas, and Tunisia): Journal of Sedimentary Petrology, v. 54, p. 1097–1109.

Tandon, S.K., and Friend, P.F., 1989, Near-surface shrinkage and carbonate replacement processes, Arran Cornstone Formation, Scotland: Sedimentology, v. 36, p. 1113–1126.

Tucker, M.E., Calvet, F., and Hunt, D., 1993, Sequence stratigraphy of carbonate ramps: systems tracts, models and applications to the Muschelkalk carbonate platforms of eastern Spain, *in* Posamentier, H.W., Summerhayes, C.P., Haq, B.U., and Allen, G.P., eds., Sequence Stratigraphy and Facies Associations: International Association of Sedimentologists, Special Publication 18, p. 397–415.

Vera, J.A., and de Cisneros, C.J., 1993, Paleogeographic significance of black pebbles (Lower Cretaceous, Prebetic, Southern Spain): Palaeogeography, Palaeoclimatology, Palaeoecology, v. 102, p. 89–102.

Verrecchia, E.P., Freytet, P., Verrecchia, K.E., and Dumont, J.L., 1995, Spherulites in calcrete laminar crusts: biogenic $CaCO_3$ precipitation as a major contributor to crust formation: Journal of Sedimentary Research, v. 65, p. 690–700.

Whitton, B.A., 1987, The biology of the Rivulariaceae, *in* Fay, P., and Baalen, C.V., eds., The Cyanobacteria: Amsterdam, Elsevier, p. 513–534.

Wieder, M., and Yaalon, D.H., 1974, Effect of matrix composition on carbonate nodule crystallization: Geoderma, v. 11, p. 95–121.

Wieder, M., and Yaalon, D.H., 1982, Micromorphological fabrics and development stages of carbonate nodular forms related to soil characteristics: Geoderma, v. 28, p. 203–220.

Williamson, W.C., 1880, On the organization of the fossil plants of the Coal Measures, Part X—Including an examination of the supposed radiolarians of the Carboniferous rocks: Royal Society (London), Philosophical Transactions, v. 171, p. 493–539.

Wright, V.P., 1985, Algal marsh deposits from the Upper Jurassic of Portugal, *in* Toomey, D.F., and Nitecki, M.H., eds., Paleoalgology: Contemporary Research and Applications: Berlin, Springer-Verlag, p. 330–341.

Wright, V.P., 1988, A micromorphological classification of fossil and recent calcic and petrocalcic microstructures, *in* Douglas, L.A., ed., Soil Micromorphology: A Basic and Applied Science, Proceedings of the International Working Meeting on Soil Micromorphology, San Antonio: Amsterdam, Elsevier, Developments in Soil Science 19, p. 401–407.

Wright, V.P., and Peeters, C., 1989, Origins of some Early Carboniferous calcrete fabrics revealed by cathodoluminescence: implications for interpreting the sites of calcrete formation: Sedimentary Geology, v. 65, p. 345–353.

Received 21 March 2005; accepted 30 June 2005.